



**ΠΑΝΕΠΙΣΤΗΜΙΟ ΠΑΤΡΩΝ**

**ΤΜΗΜΑ ΜΗΧΑΝΟΛΟΓΩΝ ΚΑΙ ΑΕΡΟΝΑΥΠΗΓΩΝ ΜΗΧΑΝΙΚΩΝ**

**ΕΦΑΡΜΟΣΜΕΝΗΣ ΜΗΧΑΝΙΚΗΣ, ΤΕΧΝΟΛΟΓΙΑΣ ΥΛΙΚΩΝ &  
ΕΜΒΙΟΜΗΧΑΝΙΚΗΣ**

**ΕΡΓΑΣΤΗΡΙΟ ΤΕΧΝΙΚΗΣ ΜΗΧΑΝΙΚΗΣ ΚΑΙ ΤΑΛΑΝΤΩΣΕΩΝ**

**ΣΠΟΥΔΑΣΤΙΚΗ ΕΡΓΑΣΙΑ**

**ΠΑΡΑΣΚΕΥΗ ΑΙΣΘΗΤΗΡΩΝ ΠΑΡΑΜΟΡΦΩΣΗΣ ΜΕ ΤΗ ΜΕΘΟΔΟ  
ΤΗΣ ΗΛΕΚΤΡΟΪΝΟΠΟΙΗΣΗΣ**

**ΑΘΗΝΑ-ΜΑΡΙΑ ΘΕΟΧΑΡΗ-ΑΘΑΝΑΣΑΚΗ**

1075458

**Κωστόπουλος Βασίλειος, Καθηγητής**

ΠΑΤΡΑ, Φεβρουάριος 2024

Πανεπιστήμιο Πατρών, Τμήμα Μηχανολόγων και Αεροναυπηγών  
Μηχανικών  
Αθηνά-Μαρία Θεοχάρη-Αθανασάκη  
© 2024 – Με την επιφύλαξη παντός δικαιώματος



---

Η έγκριση της διπλωματικής εργασίας δεν υποδηλοί την αποδοχή των γνώμών του συγγραφέα. Κατά τη συγγραφή τηρήθηκαν οι αρχές της ακαδημαϊκής δεοντολογίας.

## Παρασκευή αισθητήρων παραμόρφωσης με τη μέθοδο της ηλεκτροϊνοποίησης

Αθηνά-Μαρία Θεοχάρη-Αθανασάκη

### ΠΕΡΙΛΗΨΗ

Τα τελευταία χρόνια, υπάρχει αυξανόμενο ενδιαφέρον για την κατανόηση, την ανάλυση και την παρακολούθηση βιολογικών σημάτων και ως εκ τούτου υπάρχει ανάγκη για την κατασκευή βιοσυμβατών, λεπτών αισθητήρων ακριβούς μέτρησης. Με βάση τη βιβλιογραφία, μία από τις απλούστερες μεθόδους για την κατασκευή αυτών των τύπων αισθητήρων είναι η μέθοδος Ηλεκτροϊνοποίησης. Σε αυτή τη μελέτη διερευνώνται οι εξελίξεις στις μεθόδους κατασκευής των εύκαμπτων αισθητήρων παραμόρφωσης που κατασκευάζονται με τη μέθοδο ηλεκτροϊνοποίησης και οι βελτιστοποιήσεις στην απόδοσή τους. Οι διάφοροι τύποι εύκαμπτων αισθητήρων παραμόρφωσης, ανάλογα με τον μηχανισμό μετατροπής των δεδομένων παραμόρφωσης σε ηλεκτρικά σήματα, τις διαφορές τους, και τις εφαρμογές τους αναλύονται και αξιολογούνται ανάλογα. Οι ίνες κατασκευασμένες με τη μέθοδο της ηλεκτροϊνοποίησης έχουν μοναδική μορφολογία και προσαρμοστικές ιδιότητες, χαρακτηριστικά που τις αναδεικνύουν ως πολλά υποσχόμενα υλικά για την ανάπτυξη αισθητήρων παραμόρφωσης για διάφορες εφαρμογές. Αυτή η βιβλιογραφική ανασκόπηση εισάγει μια εις βάθος ανάλυση των τεχνικών ηλεκτροϊνοποίησης, συμπεριλαμβανομένων των παραμέτρων του διαλύματος, των επιλογών πολυμερών, και μεθοδολογίες της μετέπειτα επεξεργασίας, τονίζοντας την άμεση επίδραση στις μηχανικές και ηλεκτρικές ιδιότητες των αισθητήρων.

Λέξεις κλειδιά

Ηλεκτροϊνοποίηση- Ευέλικτοι αισθητήρες παραμόρφωσης- Πιεζοαντιστατικοί αισθητήρες παραμόρφωσης- Δομές νανοϊνών- Ενεργά νανοϋλικά



## **Development of strain-sensors by using the electrospinning process technique**

**Athina-Maria Theochari-Athanasaki**

### **ABSTRACT**

During the last few years, a growing interest that is related to understanding, analyzing, and monitoring biological signals exists, which leads to an increasing need for the fabrication of accurate and biocompatible, thin sensors. Based on the literature, one of the simplest methods to construct these types of sensors is the Electrospinning method. This study investigates the advances in flexible strain sensors fabricated with the electrospinning method and offers a comprehensive literature review of the current state of research in the wearable and flexible electronics. Multiple types of flexible strain-sensors depending on their transduction mechanism, differences, and applications are discussed and further accordingly evaluated. Electrospun fibers hold a unique morphology and adaptive properties, are considered as promising materials for developing strain sensors for a wide range of applications. This review introduces an in-depth analysis of electrospinning techniques, including solution parameters, polymer selections, and post-processing methodologies, highlighting the direct impact on the mechanical and electrical properties of the sensors.

Keywords:

Electrospinning- Flexible Strain Sensors- Piezoresistive strain sensors- Nanofiber Structures- Active nanomaterial



## LIST OF TABLES

TABLE 1: TRADE-OFF FOR TRANSITION MECHANISM OF THE STRAIN-SENSORS .....	11
TABLE 2: TRADE-OFF FOR THE ACTIVE-MATERIAL COATING METHODS.....	49



## LIST OF FIGURES

FIGURE 1: TYPES OF FLEXIBLE STRAIN SENSORS DEPENDING ON THEIR TRANSITION MECHANISM .....	2
FIGURE 2: PHASES OF THE CONSTRUCTION OF A CAPACITIVE STRAIN SENSOR PDMS/CNT ON PET FRAME, SOURCE: [7].....	4
FIGURE 3: PIEZOELECTRIC SENSOR CONSTITUTIVE PARTS, SOURCE: [9] .....	5
FIGURE 4: WORKING PRINCIPLES OF A TRIBOELECTRIC SENSOR, SOURCE: [12] 6	6
FIGURE 5: MAGNETIC STRAIN SENSOR'S FABRICATION PROCESS AND PERFORMANCE, SOURCE: [16] .....	7
FIGURE 6: CONSTITUTIVE PARTS OF A TPU/CNT@AGNW PIEZORESISTIVE STRAIN SENSOR, SOURCE: [17].....	8
FIGURE 7: TRANSDUCTION MECHANISMS OF (A) PIEZORESISTIVE STRAIN SENSORS, (B) CAPACITIVE STRAIN SENSORS, (C) PIEZOELECTRIC STRAIN SENSORS, SOURCE: [18].....	10
FIGURE 8: (A) THE CLEAR SEPERATION BETWEEN THE ISLANDS AND THE BRIDGE-MICROCRACK IS DISPLAYED IN THIS SEM IMAGE, (B) A SEM IMAGE OF THE INTERCONNECTED CONDUCTIVE NETWORK OF FIBERS, (C) THE YAMADA MODEL, SOURCE: [17] .....	13
FIGURE 9: CONFIGURATION OF MAGNETO-ELECTROSPINNING, SOURCE: [22].	18
FIGURE 10: THE SIMPLEST CONFIGURATION OF SOLUTION ELECTROSPINNING, SOURCE: [23] .....	19
FIGURE 11: (A) CRITICAL POINT IMAGE BEFORE THE FORMATION OF THE JET ANGLE OF 49.3°, (B) FORMATION OF JET [25].....	21
FIGURE 12: INFLUENCE OF SURFACE TENSION ON THE FORMATION OF THE CHARGED JET, SOURCE: [23].....	22
FIGURE 13: ILLUSTRATION OF THE STAGES OF THE CHARGED JET MOVEMENT, SOURCE: [24] .....	23
FIGURE 14: VARIOUS FIBER MORPHOLOGIES AND PATTERNS, SOURCE: [5] .....	25
FIGURE 16: ONE-DIRECTIONAL NANOYARN TYPES IN A,C,E, SEM IMAGES OF THE NANOYARNS IN B,D,F ACCORDINGLY, SOURCE: [27].....	26
FIGURE 17 SCHEMATIC ILLUSTRATIONS OF THE RING'S SIZE AND MAXIMUM APPLICABLE ADJUST HEIGHT ON THE RADIUS OF THE DEPOSITION AREA. THE RING DISTANCE FROM THE NOZZLE AND RING DIAMETER WAS (A) 1 AND 2, (B) 2 AND 4, AND (C) 3 AND 6 CM, RESPECTIVELY (YOUSEFZADEH, 2010) [28] .....	27
FIGURE 18: SINGLE WATER BATH COLLECION METHOD, SOURCE: [29].....	28
FIGURE 19: DOUBLE ELECTRODE DISC-TWISTING ELECTROSPINNING DEVICE, SOURCE: [5] .....	28
FIGURE 20: SELF-COLLECTING SPINNING TECHNIQUE, SOURCE: [30].....	29
FIGURE 21: PARAMETERS AFFECTING THE ELECTROSPINNING PROCESS, SOURCE: [33] .....	33
FIGURE 22: CONDUCTIVE POLYMERS IN FLUID FORM USED IN ELECTROSPINNING FOR THE CONSTRUCTION OF STRAIN SENSORS, SOURCE: [35] .....	36

FIGURE 23: AN EXAMPLE OF CARBONIZATION OF A POLYMER FIBER MAT, SOURCE: [36] .....	37
FIGURE 24: WORKING PRINCIPLES OF THE CONDUCTIVE PATH THAT IS CREATED DUE TO THE CONDUCTIVE FILLERS IN AN INSULATING MATRIX, SOURCE: [35] .....	38
FIGURE 25: TEM IMAGE OF CUO NANOPARTICLES IN PLGA/CUO ELECTROSPUN NANOFIBERS, SOURCE: [37] .....	38
FIGURE 26 SEM OF PURE PVDF NANOFIBER MEMBRANE DP8 COMPOSITE MEMBRANE AND ELECTROSPRAYED DP8-X WITH DIFFERENT SIO2 CONTENT. (A-A2) PVDF, (B-B2) DP8, (C-C2) DP8-0.5% SIO2, (D-D2) DP8-1.0% SIO2 [ZHANG ET AL 2022]. SOURCE: [37] .....	39
FIGURE 27: (A) CHEMICAL VAPOR DEPOSITION COATING METHOD,(B) CARBONIZATION, SOURCE: [38].....	41
FIGURE 28: IN SITU POLYMERIZATION OF HOLLOW PPY/AUNP FIBERS, SOURCE: [39] .....	42
FIGURE 29: SCHEMATIC DIAGRAM FOR FABRICATION OF AGNW-FTCF BY MEYER ROD [40] .....	43
FIGURE 30: ILLUSTRATION OF DROP-CASTING COATING, SOURCE: [41].....	43
FIGURE 31: DEPICTION OF THE DIP COATING PROCESS, SOURCE: [42] .....	44
FIGURE 32: ILLUSTRATION OF THE SPRAY METHOD PROCESS, SOURCE: [43]..	44
FIGURE 33: ILLUSTRATION OF THE SPIN COATING METHOD, SOURCE: [41].....	45
FIGURE 34: INKJET PRINTING METHOD, SOURCE: [44] .....	45
FIGURE 35: SCHEMATIC DEPICTION OF THE CONFIGURATION FOR THE THERMAL EVAPORATION COATING METHOD, SOURCE: [45] .....	46
FIGURE 36: SCHEMATIC ILLUSTRATION OF THE SPUTTER COATING METHOD CONFIGURATION, SOURCE: [46].....	47
FIGURE 37: ILLUSTRATION OF A VACUUM FILTRATION DEPOSITION METHOD WITH FILTRATION LAYERS, SOURCE: [47] .....	48



## SYMBOLS AND ABBREVIATIONS

C: capacitance	CNT: Carbon Nanotube
$\epsilon_0$ : vacuum permittivity	PTFE: Polytetrafluoroethylene
$\epsilon_r$ : relative permittivity	MWCNT: Multi-walled carbon nanotubes
A: cross-sectional area	MAPCN: Nickel nanoparticles
d: distance	AgNW: Silver Nanowire
GF: Gauge Factor	Pt: Platinum
$\epsilon$ : strain	Au: Gold
R: resistance	AC: Alternating Current
$\Delta R$ : R-R <sub>0</sub> (change of relative resistance)	DC: Direct Current
RCR: $\Delta R/R_0$	AgNP: Silver Nanoparticle
$\rho$ : resistivity factor/ density	PVDF: Polyvinylidenedifluoride
m <sub>e</sub> : electron mass	PVAc: Polyvinylacetate
h: Plank's constant	PAN: Polyacrilonitrile
p <sub>e</sub> : electrostatic pressure	PI: Polyimide
p <sub>c</sub> : capillary pressure	PDMS: Polydimethylsiloxane
$\gamma$ : surface tension	PET: Polyethyleneterephthalate
$\sigma$ : surface stress/ conductivity	DA: Dopamine
I: current	PU: Polyurethane
Q: flow rate	TPU: Thermoplastic polyurethane
K: electrical conductivity	PS: Polystyrene
E: strength of electric field	DMF: Dimethylformamide
X: volume fraction	THF: Tetrahydrofuran
$\Delta Y_{max}$ : linearity factor	DMSO: Dimethylsulfoxide
DH: hysteresis factor	HFIP: Hexafluoroisopropanol
RS: Rotational Speed	PANI: Polyaniline
TEM: Transmission Electron Microscopy	PT: Polythiophene
SEM: Scanning Electron Microscopy	PA: Polyamide
ITO: Indium tin oxide	PPy: Polypyrrole
MOS <sub>2</sub> : Molybdenum disulfide	PEDOT: Poly(3,4-ethylene dioxythiophene)
LM: Liquid Metals	P3HT: Poly(3-hexylthiophene)
IL: Ionic Liquids	PtNP: Platinum Nanoparticle
CVD: Chemical Vapor Deposition	CB: Carbon Black
ZnO: Zinc Oxide	CT: Carbon Cloth
	GO: Graphene Oxide
	CuNW: Copper Nanowire



## TABLE OF CONTENTS

ΠΕΡΙΛΗΨΗ.....	v
ABSTRACT .....	vii
LIST OF TABLES .....	ix
LIST OF FIGURES.....	xi
SYMBOLS AND ABBREVIATIONS .....	xiv
INTRODUCTION.....	1
1. FLEXIBLE STRAIN SENSORS .....	2
2.1 TYPES OF FLEXIBLE STRAIN SENSORS.....	2
2.1.1 CAPACITIVE SENSORS.....	3
2.1.2 PIEZOELECTRIC SENSORS .....	5
2.1.3 TRIBOELECTRIC SENSORS.....	6
2.1.4 MAGNETIC SENSORS .....	7
2.1.5 PIEZORESISTIVE SENSORS .....	8
2.2 TRADE-OFF.....	11
2. WORKING PRINCIPLES OF PIEZORESISTIVE STRAIN SENSORS.....	12
3.1 GEOMETRICAL EFFECTS .....	12
3.2 CRACK PROPAGATION MECHANISM .....	12
3.3 TUNNELING EFFECT.....	14
3.4 OPTIMIZATION .....	15
3.4.1 SENSITIVITY .....	15
3.4.2 LINEARITY.....	15
3.4.3 HYSTERESIS .....	16
3. ELECTROSPINNING METHOD .....	18
4.1 CONFIGURATION AND PROCESS.....	19
4.1.1 CHARGED JET FORMATION .....	20
4.1.2 TAYLOR CONE .....	23
4.1.3 SOLIDIFICATION .....	24
4.1.4 DEPOSITION OF FIBERS .....	25
4.2 FIBER MORPHOLOGY .....	25
4.2.1 ONE-DIRECTIONAL .....	25
4.2.2 TWO-DIRECTIONAL .....	29
4.2.3 COMPOSITE STRUCTURES .....	31
4.3 PARAMETERS AFFECTING ELECTROSPINNING.....	32
4.3.1 FLUCTUATIONS OF THE ELECTRIC FIELD .....	32
4.3.2 ENVIRONMENTAL FACTORS.....	32

---

4.3.3 MATERIAL PROPERTIES .....	32
4. MATERIALS USED IN ELECTROSPINNING FOR FLEXIBLE STRAIN SENSORS	34
5.1 SOLVENTS .....	34
5.2 POLYMERS .....	35
5.2.1 CONDUCTIVE POLYMERS.....	35
5.2.2 CARBONIZATION OF POLYMERS.....	37
5.2.3 BLENDING ACTIVE NANOPARTICLES IN THE ELECTROSPINNING SOLUTION.....	38
5.2.4 COATING POLYMERS WITH ACTIVE NANOPARTICLES .....	39
5. METHODS FOR COATING ELECTROSPUN NANOFIBERS WITH ACTIVE NANOMATERIALS .....	40
6.1 CHEMICAL VAPOR DEPOSITION .....	41
6.2 IN SITU POLYMERIZATION.....	42
6.3 MEYER ROD .....	43
6.4 DROP CASTING .....	43
6.5 DIP COATING .....	44
6.6 SPRAY METHOD .....	44
6.7 SPIN COATING METHOD.....	45
6.8 PRINTING METHOD.....	45
6.9 THERMAL EVAPORATION COATING METHOD.....	46
6.10 SPUTTER COATING METHOD.....	47
6.11 VACUUM FILTRATION DEPOSITION METHOD.....	48
6.12 TRADE OFF.....	48
CONCLUSION.....	50
REFERENCES .....	51
APPENDIX .....	57



## INTRODUCTION

As technology advances, it is deemed highly important to accurately obtain the optimal amount of information, in order to understand and interpret the physical changes in numerical terms. Strain sensors convert data of various types of deformation into changes in electrical signals. In a pursuit to detect the slightest deformations, flexible strain sensors have been developed, by utilizing lightweight structures from natural or synthetic polymer for applications in medicine, healthcare, robotics etc. Electrospinning is a simple and versatile technique to construct multiple types of fiber formations from polymer materials that can either be implemented on the flexible strain sensor layout or, by creating the appropriate structure, to constitute the strain sensor itself. Strain sensors created by electrospun fibers exhibit significant physical and mechanical properties; they are lightweight, flexible, breathable and durable, which make them highly desirable in biomonitoring, human-machine interaction and motion detection. In the first part of this review, differences in flexible strain sensor types and their applications are discussed, with emphasis on the piezoresistive strain sensors working principles and performance optimizations. In the second part, the electrospinning method is analyzed in depth and the different fiber patterns and their influence on the mechanical and electrical properties of the sensor are briefly described. In the third and last part, the focus is on the effect of different materials in order to obtain conductive nanofibers for the implementation into the sensor structure.

## 1. FLEXIBLE STRAIN-SENSORS

In the recent years, tracking the physical activity of one and its vital health indicators, has been proven very important, since health and medicine sectors advance. Due to this fact, there has been an increasing need for wearable, flexible sensors, which provide this information in a non-invasive way, and are highly resistant to the wear and tear of time. Flexible strain sensors can detect the dynamic traits of a physical state by transforming different types of deformation into changes in electrical signals [1]. They are lightweight, cost-effective, and have simple structures, addressing a variety of applications. Their high sensitivity and stretchability make them optimal choices for uses in human health monitoring, athletic feedback, robotics, and human-machine interfaces. The most common set-up of such strain sensors consists of a sensitive element, an electrode couple, and some wires. They are designed to detect external strain input signals and through a transition mechanism translate them into current, as the output signal.

### 2.1 TYPES OF FLEXIBLE STRAIN-SENSORS

There are certain types of transition mechanisms, the most common of which are capacitance, piezoelectricity, triboelectricity, magnetism, and piezoresistivity [2] [3].

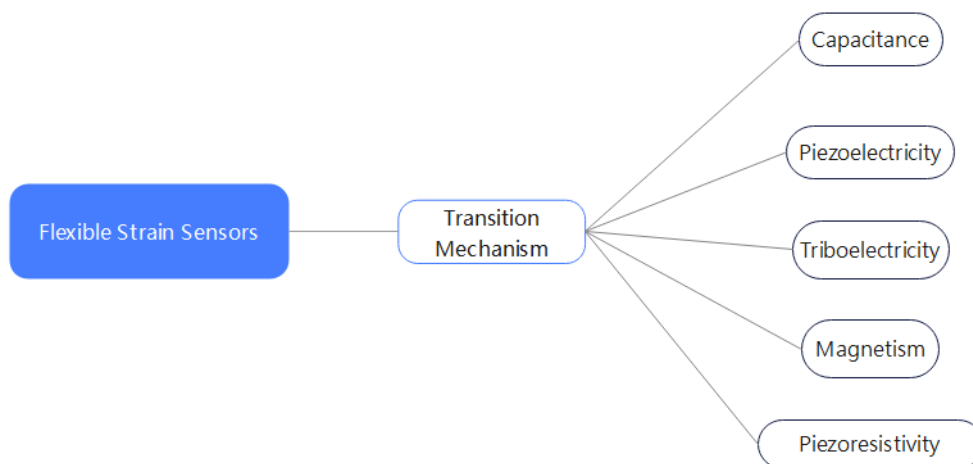


Figure 1: Types of flexible strain sensors depending on their transition mechanism

### 2.1.1 CAPACITIVE SENSORS

Capacitive strain sensors are one of the most used types. Capacitance (C), which is the phenomenon that explains their working principles, measures the charge storage between two parallel plates or a dielectric layer and can be expressed as:

$$C = \varepsilon_0 * \varepsilon_r * \frac{A}{d},$$

where A is the area of the two plates,  $\varepsilon_0$  is the vacuum permittivity,  $\varepsilon_r$  is the relative permittivity, and d is the distance between the two plates or the thickness of the dielectric layer [4]. Capacitance increases when after being subjected to stretch, the dielectric layer decreases [5]. These principles can be applied to create wearable strain sensors using nanomaterials to detect capacitive strain. The Gauge Factor (GF) estimates the sensitivity of the strain sensor and is calculated by the equation:

$$GF = \frac{\Delta C}{C_0 * \varepsilon}$$

where,  $C_0$  is the capacitance of strain sensors in an unstretched state, where  $\Delta C$  is the change of capacitance between the stretched and the initial state, and  $\varepsilon$  is the strain [6].

The Poisson's Ratio is also a very important characteristic number for each material as it relates the changes in deformation in the transverse(lateral) with the deformation in the axial (longitudinal) direction. Usually, materials have a positive Poisson ratio. While an axial expansion moves active materials away from each other in the substrate, contact resistance is reduced. and a volume compression in the transverse direction brings the active materials closer. Resistance increases due to axial tension but is equalized by the transverse Poisson compression, which in turn lowers the resistance change and sensitivity of the sensor. To tackle the latter effects, metamaterials with negative Poisson ratios are being studied for possible utilization in the future [5].

In his study, Lee et al introduced a new capacitive strain sensor using CNTs, with a strain range of 1% to 300% that exhibits good endurance. The sensor demonstrates great sensitivity as well as a linear capacitive relation [7]. In the same way, a pressure sensor built on textiles was created [8]. Silver nanoparticles were integrated into an

elastic rubber shape to create this sensor. It demonstrated a good sensitivity of  $0.21 \text{ kPa}^{-1}$ , stability of over ten thousand cycles, and reaction times of less than 10 milliseconds. Given that it can be incorporated into gloves and clothing, this sensor has great promise for the textile industry.

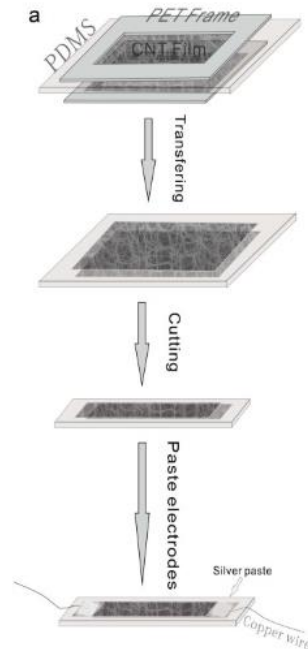


Figure 2: Phases of the construction of a capacitive strain sensor PDMS/CNT on PET frame, Source: [7]

### 2.1.2 PIEZOELECTRIC SENSORS

Piezoelectric sensors are powered by the electrical signals caused by the piezoelectric effect, which is the ability of specific materials to produce an electrical charge due to imposed mechanical stress. Piezoelectric materials, such as lead zirconate titanate (PZT), lead titanate, and barium titanate, convert vibrations into electrical signals and subsequently they can be used as strain sensors [2]. Ghosh et al created flexible sensors out of nanofibers composed of fish gelatin using electrospinning. The sensors produced are cost-effective, lightweight, versatile, and environmentally friendly. With a lifetime of up to six months, the flexible sensors power their operations and imitate human experiences because of the stability and enhanced mechano-sensitivity of these nanofibers [12].

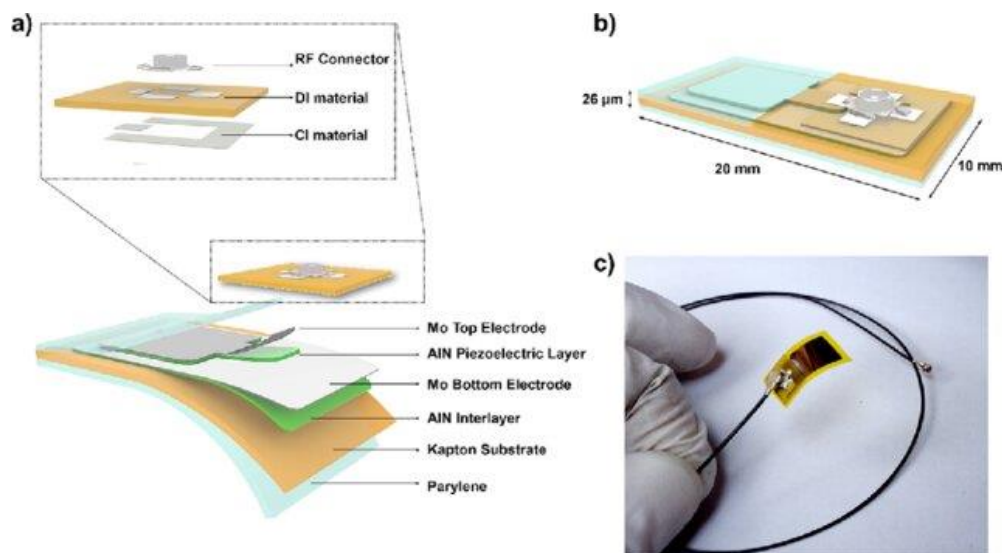
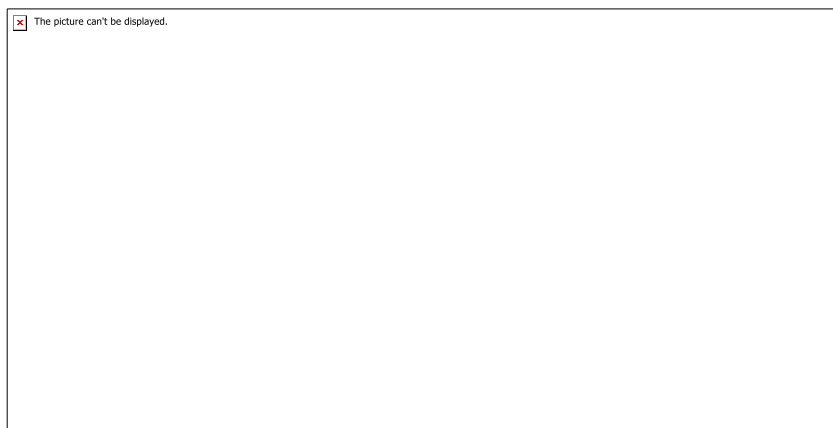


Figure 3: Piezoelectric Sensor Constitutive Parts, Source: [9]

### 2.1.3 TRIBOELECTRIC SENSORS

The effect known as triboelectricity is the electrification of incompatible objects or materials occurring by a collision that causes a phenomenal flow of electrons from one material to another, therefore balancing the potential difference. Triboelectric sensors are self-powered and utilized in applications such as soft robotics, wearable electronics, and for power purposes [10] [11]. The triboelectric output is caused by the coupling of the triboelectric effect and the electrostatic induction under a mechanical strain input, that is converted into electrical signals. Triboelectric nanogenerators consist of four layers of materials that have the appropriate traits, the charge-generating layer, the charge-trapping layer, the charge-collecting layer, and the contact layer. The number of electrical signals attained, relies on various conditions of the mechanical interference, including time and area [12]. Zhou et al. proposed an active fiber-based strain sensor composed of two types of pretreated cotton threads: CNT-coated cotton thread and PTFE and CNT-coated cotton thread. The two types of threads are entangled to form a double helix and then coiled around a silicone. The amount of transferred charges between the two threads varies linearly with the changed stimulated strains and can avoid the influence of the stimulated frequencies. This sensor can detect up to 25% strain, thereby demonstrating the finger motion states [13] [14].



*Figure 4: Working Principles of a triboelectric sensor, Source: [12]*

#### 2.1.4 MAGNETIC SENSORS

Magnetism is the phenomenon that associates with magnetic fields, and is caused by the motion of electric charges. Magnetic strain sensors can be fabricated when magnetic nanoparticles are incorporated into composite fibers that make up the flexible sensor to provide touchless sensing. The type and quantity of magnetic fillers have a direct impact on the magnetic induction strength. However, the use of these fillers causes low conductivity, weak strength, and severe nanoparticle clustering. Some methods have been introduced to enhance the mechanical, conductive, and magnetic properties such as chemical modification, though further research should be conducted to achieve appropriate results [15].

Ruixue Sun et al, in order to create a unique flexible strain sensor with an anisotropic structure and a broad operating range, developed an efficient approach to induce the self-assembly and placement of MWCNTs in polymer composites by a mild curing magnetic field (less than 0.7 T). By loading a tiny amount of nickel nanoparticles (MAPCN), the synergistic effect of MWCNTs and conductive particles was used to further optimize the comprehensive sensing capability. This increased the sensitivity of MAPC to tensile strain. The improved endurance and sensitivity characteristics, along with the quick response time, that were attained, enabled MAPCN to precisely track human physiological activity, and a gesture recognition system was created to highlight the technology's usefulness and possible future in wearable technology [16].

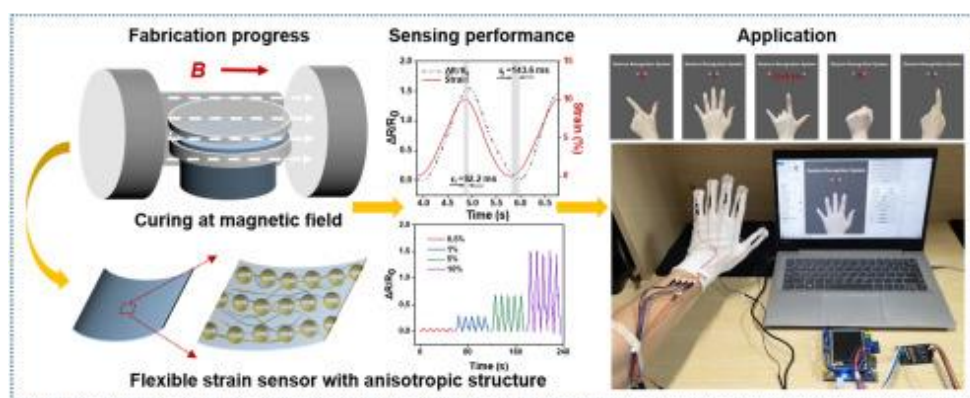


Figure 5: Magnetic strain sensor's fabrication process and performance, Source: [16]

### 2.1.5 PIEZORESISTIVE SENSORS

Piezoresistivity is the phenomenon in which stress, that is applied to a conductor or semiconductor material, generates movement in the energy valley due to changes in the energy band, without causing volume or shape alterations. Thus, the carrier mobility and the resistivity of the material change accordingly. Resistance changes caused by deformation are expressed as the piezoresistive rate. Piezoresistive strain sensors are the most commonly used flexible strain sensors however they require an external power supply to function, which makes them inappropriate for some applications. Flexible resistive strain sensors typically consist of a polymer, insulating, stretchable substrate, a conductive substrate or film, and two electrodes and some wires, as displayed in Figure 6. The silver paste is used as an adhesive for the copper electrode onto the CNT@AgNW substrate.

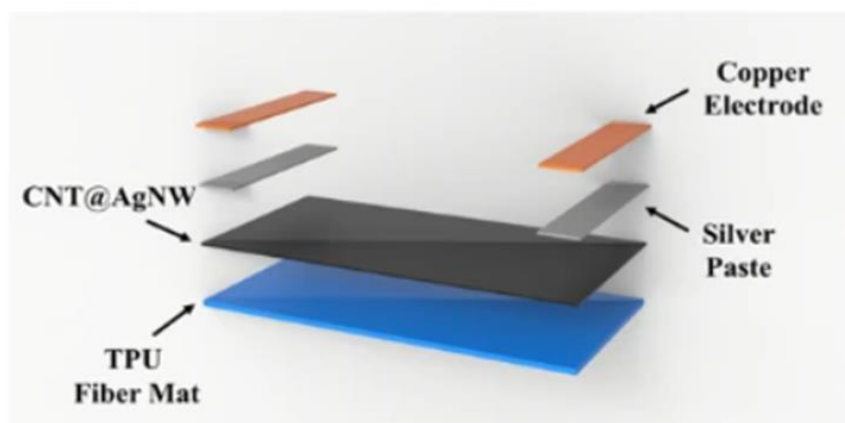


Figure 6: Constitutive parts of a TPU/CNT@AgNW piezoresistive strain sensor, Source: [17]

There are two types of piezoresistive strain sensors the positive, whose resistance is increased with strain, and the negative, whose resistance is decreased with strain. They respond quantitatively to the degree and direction of strain applied to sensors by the change in piezoresistivity (increased resistance), which is initially measured indirectly by the change in current at a certain voltage caused by the deformation of the conductive layer, and then translated into resistance.

The Gauge Factor (GF) represents the slope of the rate of change of the RCR rate, which is an expression of the relative resistance to the initial resistance  $RCR = \frac{\Delta R}{R_0}$ , to the strain  $\varepsilon$  an expresses the magnitude of sensitivity.

$$GF = \frac{R - R_0}{R_0 * \varepsilon} = \frac{\Delta R}{R_0 * \varepsilon} = \frac{RCR}{\varepsilon}$$

where R is the resistance under tension, R<sub>0</sub> the initial resistance, ΔR the change of relative resistance and ε the applied mechanical strain.

The relative change in resistance graphed against the applied strain in a strain transducer's RCR-strain curve is known as the plot of specification factors or sensitivity. A study conducted by Gong S. et al, showcased that gold nanoparticles (AuNWs) could be integrated into latex rubber to create a AuNWs/latex strain sensor. For human motion detection he made use of nanowires that ranged from two nanometers to several tens of micrometers in length, without a noticeable decrease in their mechanical flexibility. The sensors show stretchability of more than 350% for a GF of around 10%, a response time faster than 22 ms, and a tensile strain from 0.01% to 200%. These sensors can be used in monitoring limbic movements and pulses. When adjusted on a glove they can distinguish between hand position and gestures [13].

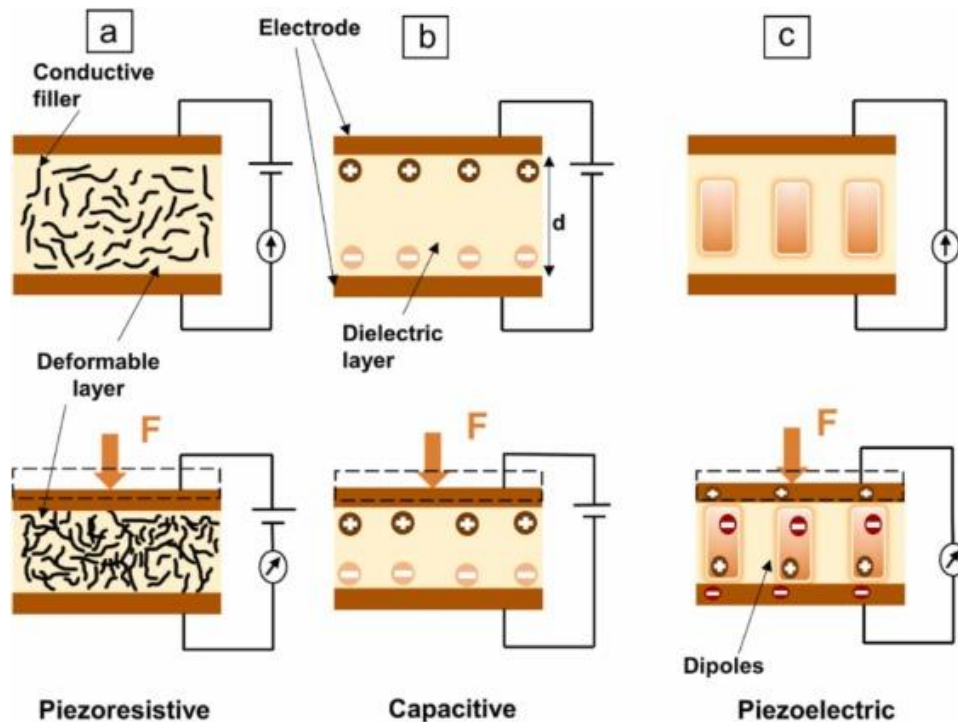


Figure 7: Transduction mechanisms of (a) piezoresistive strain sensors, (b) capacitive strain sensors, (c) piezoelectric strain sensors, Source: [18]

Figure 7 displays the working principles of the transduction mechanisms of piezoresistive, capacitive and piezoelectric strain sensors. The differences in their operations are clearly showcased. The piezoresistive strain sensor requires conductive fillers and deformable layers, the capacitive electrodes and a dielectric layer and the piezoelectric dipoles, in order to function.

## 2.2 TRADE-OFF

The following table describes a simple technique to compare the flexible strain sensors that were introduced above depending on some of their characteristics, in order to evaluate which type is appropriate for the desired application.

*Table 1: Trade-off for transition mechanism of the strain sensors*

<b>Strain Sensors</b>	<b>Sensitivity</b>	<b>Accuracy</b>	<b>Durability</b>	<b>Sensing Range</b>	<b>Fabrication Complexity</b>	<b>Transient Response Time</b>	<b>Energy consumption</b>	<b>Cost</b>	<b>Total points</b>
<b>Capacitance</b>	3	2	2	1	2	3	1	3	17
<b>Piezoelectric</b>	1	2	3	1	1	2	3	2	15
<b>Triboelectric</b>	3	2	2	3	1	3	3	1	18
<b>Magnetism</b>	1	1	2	1	2	2	2	2	13
<b>Piezoresistive</b>	3	2	2	3	2	2	1	3	18

The scoring range is from one (1) to three (3), and the highest score (3) means the optimal behavior for the characteristic. For example, a score of three for cost means that the sensor is inexpensive, and a score of one means that it is expensive. For sensitivity, three means a highly sensitive sensor and one that it is not quite sensitive. To be able to have a more accurate trade-off table, weighting coefficients can be added on the characteristics that are most important in each design. In this trade-off all characteristics are considered to have equal weighting factors. As can be observed, the triboelectric and the piezoresistive strain sensors are the highest in score, however, the first is much more complex and expensive than the latter. While cost and complexity are two crucial factors for the fabrication of the sensor in the lab, the emphasis will be given to piezoresistive strain sensors.

## 2. WORKING PRINCIPLES OF PIEZORESISTIVE STRAIN-SENSORS

A strain sensor of this type consists of a polymer substrate and a conductive substrate/film. The polymer substrate offers the sensor appropriate stretching and reversible properties, while the conductive substrate when subjected to strain, increases its resistance because of the reduction of the conductive path due to microstructural changes in the element. The conductive layer is a network of overlapping conductive pathways, depending on the given structure. The geometrical effects and inherent resistivity changes, along with a breakage mechanism- crack propagation, and a tunneling effect are the main factors that cause the piezoresistive response.

### 3.1 GEOMETRICAL EFFECTS

Concerning the geometrical effects, they depend on the materials utilized and the structure of the sensor. When a material is subjected to transverse Poisson compression under tension, it tends to expand in the axial (longitudinal) direction. Resistance in a conductive material is given by  $R = \rho * \frac{L}{A}$ , where  $\rho$ =resistivity,  $L$ =length, and  $A$ = cross-sectional area of the conductive substrate. As the length is increased or the cross-sectional area is reduced, resistance increases. Resistivity  $\rho$  is a distinct characteristic of each material.

### 3.2 CRACK PROPAGATION MECHANISM

Materials contain cracks inherently, and when stretched, the cracks propagate and breakage takes place. There might be overlapping in the conductive network, therefore allowing electrons to travel through these interconnected pathways. The interface between the polymer substrate and the conductive one may mismatch or slip, when the material is stretched, due to low friction or poor adhesion between substrates, or miss overlapping in certain areas. This translates to a reduction in the conductive pathways and an increase in contact resistance of the nanomaterials and thus the total resistance of the strain sensor.

Incorporating active agents such as Ag, Pt, CNT's, Graphene Oxide, or Au into nanofiber mats by coating and pre-stretching them, offers significant increases in

flexibility, sensitivity, and reliability of strain sensors. The process of stretching is crucial because it generates a substantial increase in the resistance of the nanofibers. Through this operation, microcracks appear and grow in the brittle coating on top of the conductive substrate, and allow further separation of the coating film from the substrate at the edge of the crack, creating two islands, separated by the crack, functioning as a bridge, which in turn leads to limited electron trade and increased contact resistance. Depending on the intensity of the stretching, the size and density of microcracks are analogous. After unloading, cracks recover and close due to shrinkage and stretching of the substrate, thus the edge conductive paths that were previously cut, are also reconnected, and conductivity is restored [5]. To further clarify this mechanism, the Yamada et al. model is introduced to reduce the resistance change of the crack structure to the following expression:

$$R' = \frac{Ra * Rc + 2 * Ra * Rb + Rb * Rc}{Ra + 2 * Rc + Rb}$$

Where  $R'$  is the resistance of a single microcrack structure;  $R_a$  is the resistance of the island;  $R_b$  is the resistance of the bridge that connects the two islands at both ends of the crack; and  $R_c$  is the resistance of the fiber loaded with the active material. It has been proved that  $R_b$  and  $R_c$  are positively correlated with strain and  $R'$  shows the changing trend of a quasi-exponential function, providing high GF to the sensor [17].

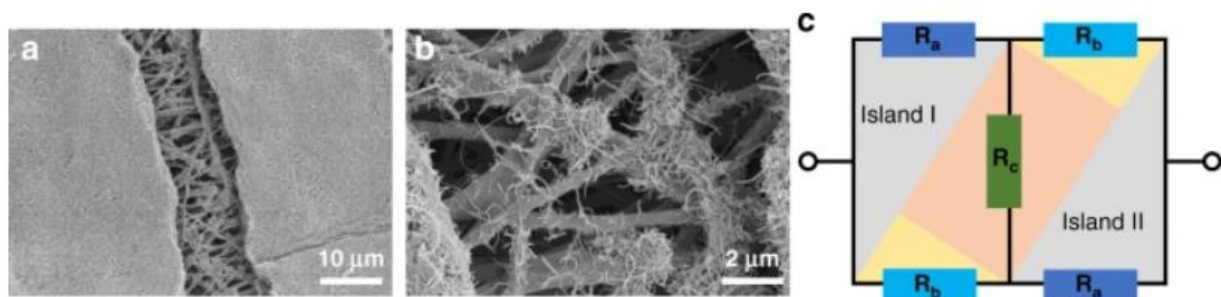


Figure 8: (a) The clear separation between the islands and the bridge-microcrack is displayed in this SEM image, (b) A SEM image of the interconnected conductive network of fibers, (c) The Yamada model, Source: [17]

### 3.3 TUNNELING EFFECT

The tunneling effect takes place when active nanomaterials are so close to each other that they form electron-conductive paths that surpass the insulating polymer substrate barrier. Based on Simmon's tunneling theory, the total resistance  $R_t$  is obtained from the following equation:

$$R_t = \frac{8\pi h d}{3s r e^2} \exp(r d), r = \frac{4\pi}{h} \sqrt{2m_e * \varphi}$$

where  $h$  was the Plank's constant,  $s$  was the effective cross section,  $e$  was the electron charge,  $d$  was the average distance between adjacent conductive nanofillers,  $m_e$  was the electron mass and  $\varphi$  was and the height of tunneling potential barrier, respectively [1].

For further understanding of the topic, an example of CNT's polymer composite will be discussed [19]. The piezoresistive behavior of this material happens, either because of a change in the dimension of the individual CNTs or because of the deformation of the conductive network of CNTs.

- a. The dimensional change happens due to inherent piezoresistive behavior and geometrical effects
- b. The deformation of the conductive network depends on the distance between the adjacent CNTs. When the distance is increased there is an increase in the contact resistance and a decrease in the conductivity of the conductive path, reaching insulation at the maximum tunneling distance, which depends on the composite and the process it is subjected to.

For CNT's strain sensors, the tunneling effect is dominant for both axial and transverse directions, but the piezoresistive effect only plays an important role in the transverse direction, not the axial [5].

### 3.4 OPTIMIZATION

The performance of flexible strain sensors can be measured by multiple parameters. It is either influenced by the sensor's response traits, such as the sensitivity (or Gauge Factor-GF), linearity, hysteresis that is affected by response time, and recovery time, or by its structural characteristics. These include the type, substance, and structure of the active component, the type and structure of the substance material, and their interlaminar compatibility.

#### 3.4.1 SENSITIVITY

Sensitivity, which is expressed quantitatively as the GF, is one of the most essential metrics used to assess sensor performance. It indicates the sensor's ability to detect slighter or larger changes in resistance and the response potential of the active nanomaterial due to imposed external mechanical strain. Greater sensitivity in strain sensors is a sign of greater performance, since it denotes a low limit of detection and high resolution, thus making a clear distinction between fine and larger movements. Electrospun fiber strain sensors opt to use brittle active materials along with a flexible fiber mat, while brittle conductive materials under even minor strains obtain irreversible fractures thus high GF value and significant sensitivity.

#### 3.4.2 LINEARITY

Linearity is the indicator of the consistency of measurements over the entire range of measurements. It is described as:

$$\Delta Y_{max} = 1 - R^2$$

where the percentage of the maximum deviation is  $\Delta Y_{max}$  and the relationship between the sensor calibration curve, the fitted straight line, and the full-scale output under specific conditions, exhibited as  $1 - R^2$ , which is also referred to as nonlinear error. The closer the strain sensor's measurements are to a straight line on sensitivity plots the better the quality of the sensor is. While metal strain sensors usually have a greatly linear response because of the dependence of the strain coefficient to the Poisson ratio, which is showcased by an equal proportion increase of the resistance and the strain, for flexible strain sensors this is not the case. Polymers, that are used as substrate materials, have intrinsic viscoelasticity, thus any external force applied causes inhomogeneous deformations and the sensors display a nonlinear response. Different linearity regions are typically formed depending on the different resistance

changes generated by the conductive material during the actual stretching or reversion of the sensor. The effective linearity is selected based on the stretchability of the sensor and the effective monitoring range within which, the sensor's internal structure is stable and the data is most informative [20].

### 3.4.3 HYSTERESIS

Hysteresis is the difference in value of the resistant output of a strain transducer during loading and unloading cycles, while maintaining equal strain levels. The hysteresis behavior is associated with response time, mechanical deformation and/or temperature. If the response time is short then hysteresis is weaker and the sensitivity of the sensor is higher. Regarding mechanical hysteresis it is affected by strain rate and magnitude, the conductive material's characteristics and the interlaminar bonding of the conductive and the flexible substrates. Quantitatively it is recorded as

$$DH = \frac{A_{loading} - A_{unloading}}{A_{loading}}$$

where  $A_{loading}$  and  $A_{unloading}$  are the areas of the loading and unloading curves, accordingly. A smaller value of hysteresis (DH) indicates lower hysteresis in the sensor response, thus higher sensitivity. The interactions between the different material layers make hysteresis unavoidable, however it is possible to diminish this effect by introducing additives or chemical reactions to enhance interfacial bonding and improve the sensor performance [20].

Electrospun fiber-based strain sensors' sensitivity is influenced by electrospinning preparation parameters, that will be further analyzed in Chapter 4. The needle's tip diameter and its distance from the collector, the electrospinning time, and in case the desired result is an oriented fiber mat structure, the roller collector's speed. Certain experiments have highlighted that lower collector's speed, shorter tip-to-collector distance, and a longer time electrospinning process led to the creation of more uniform fiber mats with high sensitivity and conductivity.

One experiment, conducted by Wang et al, [21] for the production of a high-performance strain sensor, using electrospinning and ultrasonication, showcased that by embedding carbon black particles in a thermoplastic polyurethane fibrous film, the sensor achieves wide stretchability, high sensitivity, and cost-effective production.

The study focuses on the impact of the rotational speed of the electrospinning collection device and discusses the results of two samples. RS-100 for 100rpm rotational speed and RS-200 for 200rpm, on the stereotypic scaffold network structures and the fiber diameter of the TPU/CB composites. It is shown that scaffold network structures were affected by the rotational speed of the collector, leading to differences in mechanical behavior of materials and that the fiber diameter and the scaffold internal area greatly influenced sensitivity under stretching conditions.

### 3. ELECTROSPINNING METHOD

Flexible strain sensors rely on specific preparation methods to achieve significant sensing performance and potential use in a variety of applications. One of the fiber preparation methods that is highly efficient is electrospinning. It is a simple, inexpensive, and adaptable method for constructing ultrathin fibers. It can create great-quality, high-porosity, homogeneous nanofibers by utilizing a wide range of materials, such as polymers, metals, and ceramics. There are specific alterations of the electrospinning method depending on the parameters of the fluid and the configuration of devices. The specific method that will be analyzed below is solution electrospinning, which is most used. To date, more than 100 different types of organic polymers, both natural and synthetic, have been successfully explored for solution electrospinning to produce continuous nanofibers directly.

Another interesting process called Magneto-electrospinning is an alternate way to construct nanofibers, but enriched with magnetic properties. It follows the same principles as solution electrospinning, however, it makes use of an electromagnet. The electromagnet is a setup consisting of a wire wrapped into a coil. When utilized in a magneto-electrospinning process, it is placed in the vicinity of the high-voltage power supply. The magnetic field configuration determines the arrangement of the coil. The current flow that runs through it generates the magnetic field and depending on its rate controls the strength of the latter. The different results in the fibers compared to those of electrospinning are that they are thinner and of uniform diameter, while also holding magnetic properties [23].

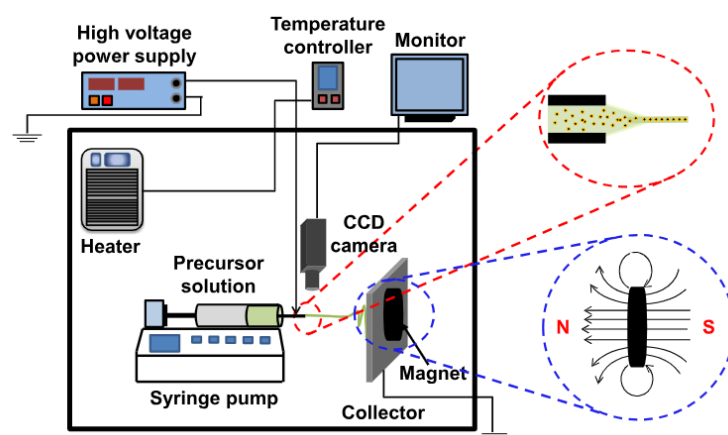


Figure 9: Configuration of Magneto-electrospinning, Source: [22]

#### 4.1 CONFIGURATION AND PROCESS

The devices and structures used for the electrospinning process are a high-voltage (some tens of kV) power supply either of Alternating Current (AC), or of Direct Current (DC), which is weak ( $10^{-7} - 10^{-3} \text{ mA}$ ) a spinneret, and a device to support the spinneret and adjust the disposal rate of the solution and a grounded collector-cathode. A spinneret is a metal device used to extrude a polymer solution to form fibers. The dispenser is filled with a viscous polymer solution or emulsion or a melted polymer, which will later on exit via the spinneret edge in droplet form into the air, leading the droplet to undergo phase inversion and solidification. The viscous flow that characterizes this process causes the individual polymer chains to align.

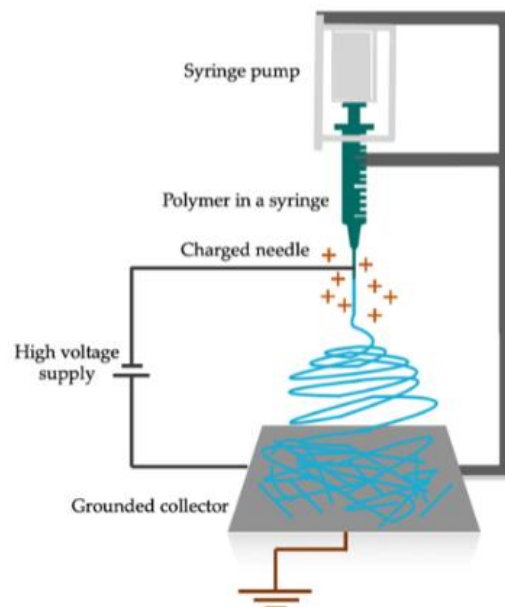


Figure 10: The simplest configuration of solution electrospinning, Source: [23]

#### 4.1.1 CHARGED JET FORMATION

The positive receptor of the power supply is connected to the spinneret and the negative to the collector. An electrostatic field of high voltage is created in the space between the needle and the collector and the transient potential increases the voltage of the fluid extruded. The droplet leans towards stabilization at the tip of the needle and forms a spherical shape, while electrostatic repulsion forces tend to surpass the surface tension, created by the distinct viscosity of the liquid. The spherical shape is created while it is optimal for the minimization of the free energy at the surface of the droplet. However, the electrostatic repulsion tends to deform the droplet shape, thus the surface area increases, due to surface tension, in order to reduce the repulsion forces. The droplet takes the ideal shape to minimize the sum of the electrostatic and the free surface energy. Under the assumption that the liquid is a perfect conductor, the electrostatic pressure ( $p_e$ ) that is applied on the droplet surface due to the external electrical load, can be calculated from the equation:

$$p_e = \frac{\varepsilon' * E^2}{2}$$

Where  $\varepsilon'$  is the dielectric constant of the mean that surrounds the droplet and E is the volume of the electric field.

The capillary pressure ( $p_c$ ) appears due to surface tension and it is characterized by Young-Laplace equation:

$$p_c = \frac{2 * \gamma}{r}$$

Where  $\gamma$  is the surface tension and r is the mean radius of curvature of the surface, which can be replaced by the needle inside radius. When the voltage rises to a certain critical voltage ( $V_c$ ) and the electric field is sufficiently strong,  $p_e$  will surpass  $p_c$ , which means that the electrostatic repulsion will surpass the surface tension. The droplet in this case is elongated, forming a Taylor cone [24] [25].

The critical voltage is calculated as:

$$V_c = \pm \sqrt{\frac{4H^2}{h^2} * \left( \ln\left(\frac{2h}{R}\right) - 1.5 \right) (1.3\pi R\gamma)(0.09)} \text{ (kV)}$$

Where H is the distance between the tip of the needle and the collector, h the length of the needle and R the radius of the needle. H,h and R have cm as their unit and the surface tension  $\gamma$  has dyn/cm (1 dyn/cm=0.001N/m). The constant 1.3 is derived from  $2*\cos(49.3^\circ)$ , while the cone is formed under the electric field only at a semi-vertical angle of  $49.3^\circ$ , as it was observed by Taylor's experiments [26].

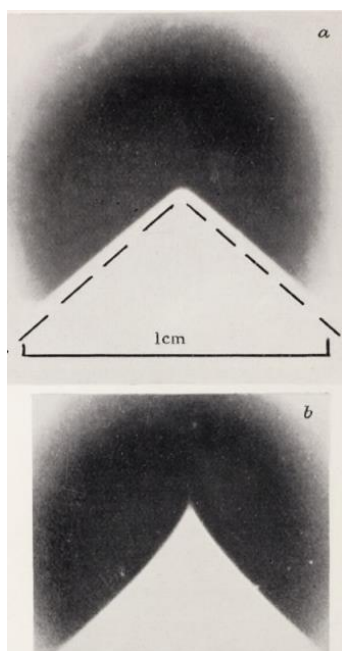


Figure 11: (a) Critical point image before the formation of the jet angle of  $49.3^\circ$ , (b) Formation of jet [25]

Depending on the polymer concentration in the solution, different results will occur. If it is too low, viscosity and surface tension have also small values, leading to electrostatic atomization, and the fluids' shape is beads or spindle fibers. In case the polymer concentration is appropriate, the solution retains its cohesion, and Rayleigh instability is suppressed due to the viscoelasticity of the fluid, which results in a charged jet, as mentioned above. If it is too high, the viscosity is prevalent, the surface tension is stronger than the localized charges, and the polymer chains are severely entangled. The fluid is concentrated in the nozzle, the droplet forms a spherical shape and the electrospinning process is hindered [5] [23].

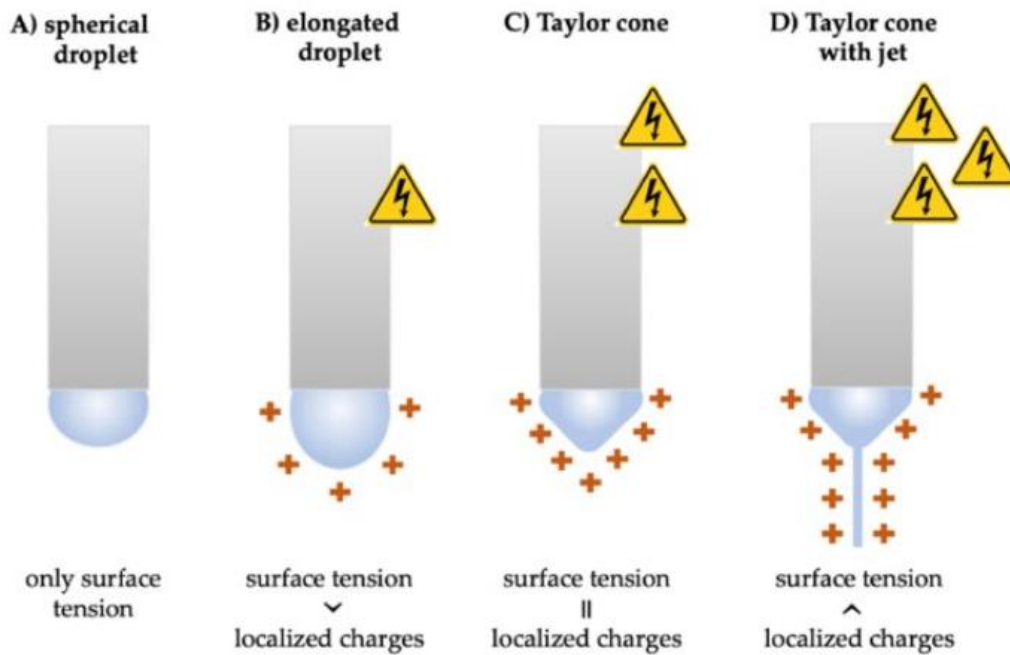


Figure 12: Influence of surface tension on the formation of the charged jet, Source: [23]

The third case is not functional, and the first better explains methods, such as electrospaying. Both will not be concerned with this matter of research.

#### 4.1.2 TAYLOR CONE

The charged jet that is formed in the second scenario, fluctuates through stable and unstable phases. During the stable ones, the solvent evaporates, the solution solidifies and is deposited as fiber spirals onto the cathode. In the unstable phase, the jet whips and splits into filaments. [5]

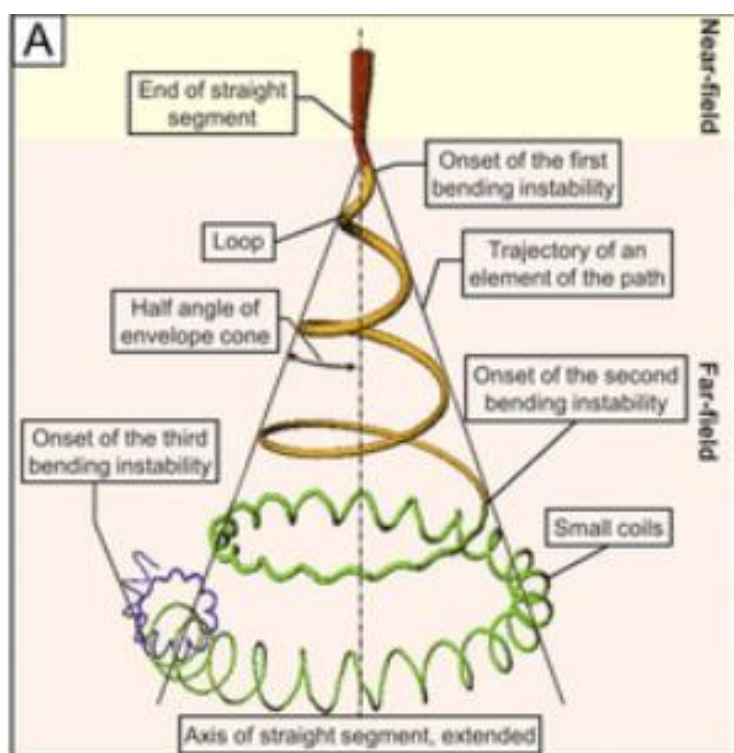


Figure 13: Illustration of the stages of the charged jet movement, Source: [24]

Various models have been discovered to describe this behavior, based on experiments and electrohydrodynamic theories. They assist in obtaining a deeper understanding of the mechanism of electrospinning and enhanced control over the parameters affecting the process and the resulting nanofibers. One model suggests that the jet's behavior resembles the one of a string of connected viscoelastic dumbbells and calculates a three-dimensional trajectory for the jet by using a linear Maxwell equation that agrees with the experimental results. Another model proposed that nonlinear rheology should be calculated in the stretching part of the jet in order to describe its motion under the electric field.

In Figure 12, it can be observed that in the first segment, which is called the near-field region, the charged jet is in a straight line. The Rayleigh instability is suppressed by the viscoelastic properties of the fluid, and the surface charges move along with the jet, generating a current. The diameter of the jet, the velocity and the length can be measured. The velocity at the end of the straight line is calculated around 1-15m/s.

The critical length of the straight line of the jet, is calculated approximately by the following equation:

$$L = \frac{4kQ^3}{\pi\rho^2 I^2} \left( \frac{1}{Ro^2} - \frac{1}{r_0^2} \right)$$

where  $Ro = \left( \frac{2\sigma Q}{\pi\rho kE} \right)^{\frac{1}{3}}$ ,  $\sigma$  is the surface stress,  $Q$  is the flow rate,  $I$  is the current passing through the jet,  $E$  is the strength of the electric field,  $k$  is the electrical conductivity of the fluid,  $\rho$  is the density of the fluid, and  $r_0$  is the initial radius of the jet.

In the following region, the Far-Field, three types of instabilities can occur. The first is axisymmetric, known also as Rayleigh instability, which is prone to causing the breakup of the jet into droplets. It can be suppressed at an intense electric field, and the surface tension is dominant. The second type is axisymmetric, similar to the first, however, it is present at a stronger electric field. The third type is non-axisymmetric, it is the whipping or bending instability and describes long wave disturbances to the jet. They are caused by the aerodynamic instability and the lateral electrostatic force in a radial direction towards the jet and lead to electrostatic repulsion between surface charges in a powerful electric field.

#### 4.1.3 SOLIDIFICATION

The jet undergoes phase transition and solidifies during the elongation process, which is caused by the evaporation of the solvent. In a slower solidification process, the elongation process lasts longer, leading to thinner fibers. After the completion of this phase transition, the surface charges remain on the dry fibers, although all the instabilities cease to exist.

#### 4.1.4 DEPOSITION OF FIBERS

The final step of the electrospinning process is the deposition of nanofibers onto a grounded collector [24]. The fiber morphology heavily relies on the device used as the collector. The different types of fibers structures will be further analyzed below.

#### 4.2 FIBER MORPHOLOGY

The electrospinning process is highly versatile, and due to this fact, it is suitable for use in multiple applications. Each application requires a different structure of substrates and, thus different fiber morphology. The electrospun nanofiber structures can be further classified as one-directional, two-directional, and distinct composite fiber structures.

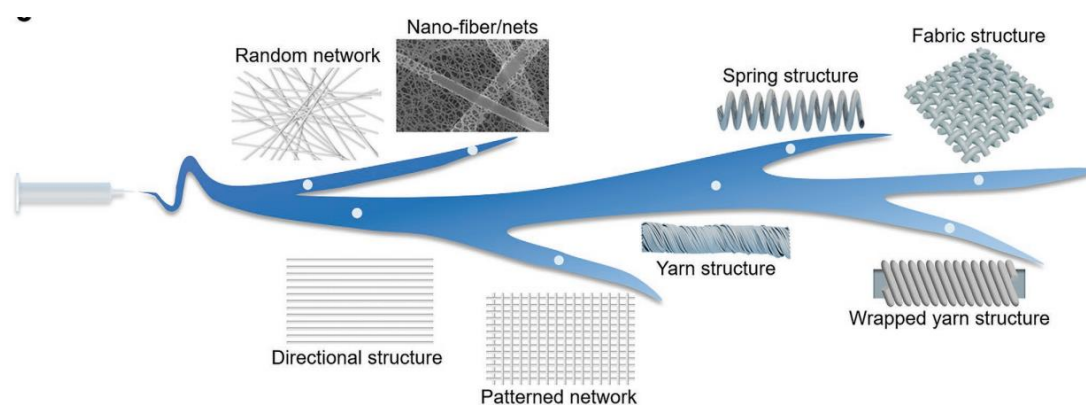


Figure 14: Various Fiber Morphologies and Patterns, Source: [5]

##### 4.2.1 ONE-DIRECTIONAL

Regarding the one-directional structure, the fibers are characterized by increased knittability, and flexibility, and light weight. They can be blended into everyday textiles or be directly woven into them, or be used as channel materials for stretchable transistors.

In order to achieve these results, the fibers should be formulated into yarn structures, whereas they provide enhanced tensile properties compared to non-woven, random settings. The latter is more suitable for continuous stretching requirements.

Yarn-shaped nanofibers can be utilized as highly sensitive strain sensors with a maximum strain larger than 50% and significant conductivity when they are enriched

with electrically conducting materials e.g. CNTs, graphene oxide, silver nanoparticles, and AgNPs via deposition.

The structures are classified as aligned yarns, twisted or spiral, and core-spun yarns.

- i. The aligned yarn consists of multiple axially aligned nanofibers along the yarn's longitudinal direction. Aligned nanofiber arrays can be created by altering conditions influencing the flow rate and the collector during electrospinning. They can be used as channel materials when they are made of conjugated polymers (polymers whose backbone chain has altering double-single bonds).
- ii. The twisted type exhibits the same structure as the aligned yarn, but the fibers are twisted together.
- iii. The core-spun yarn shape is made of a core yarn, which has a greater diameter than the outer spiral, provides elastic properties to the yarn, and supports the total structure; an outer spiral, in which the active materials are incorporated and exhibits the appropriate level of stretchability to obtain the normal function of the conductive network [27].

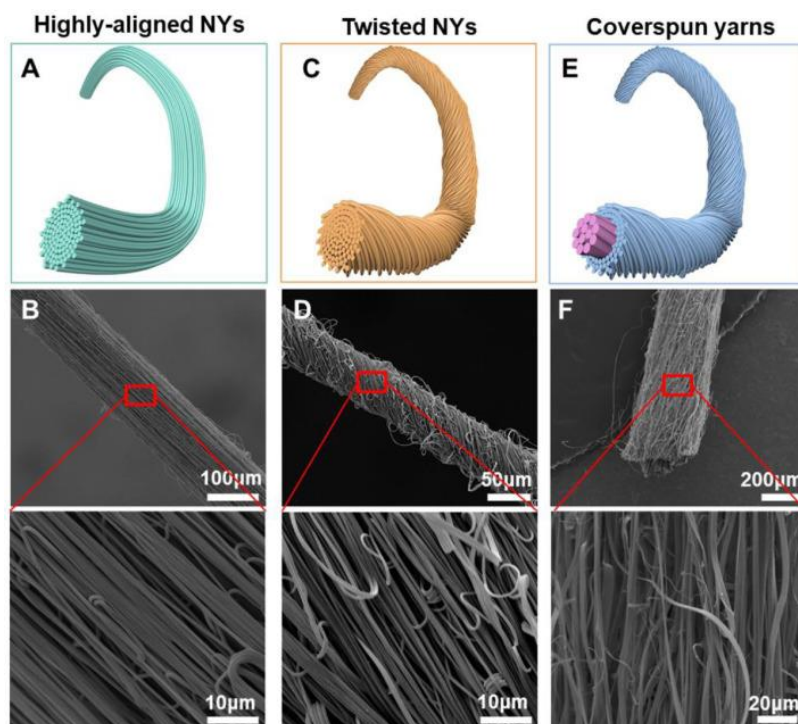


Figure 15: One-directional nanoyarn types in A,C,E, SEM images of the nanoyarns in B,D,F accordingly, Source: [27]

Different preparation methods provide different properties for the yarn. The simplest configuration to attain a nanofiber yarn is by directly electrospinning the polymer solution and then twisting it to form the desirable structure. Some require the intermediation of devices in place of the collector between the spinneret and the twisting device. These are mainly auxiliary electrode collection devices, water bath method collection and variations, double electrode disc twisting electrospinning, and self-collecting spinning devices.

- The auxiliary electrode collection device consists of a pair of electrodes with a constant gap between them or a metallic ring, which orients the fibers to form greatly aligned bundles. However, the process offers limited-length fibers and allows no further twisting [28].

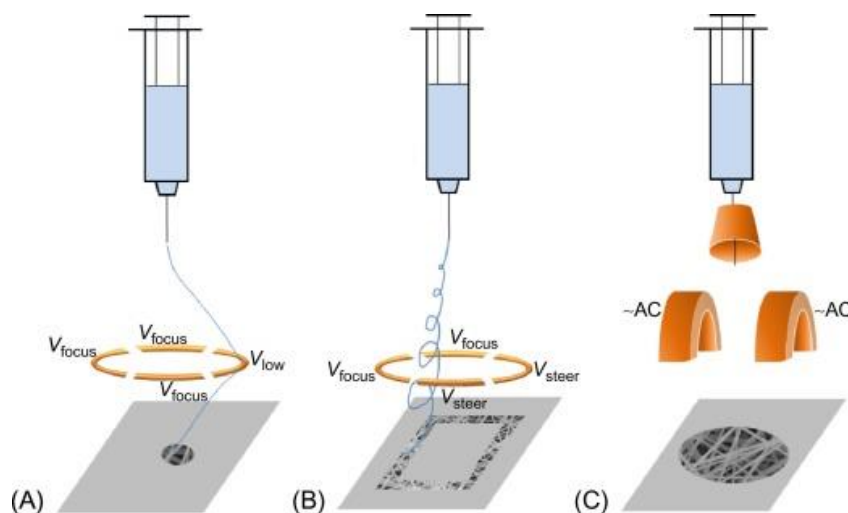


Figure 16 Schematic illustrations of the ring's size and maximum applicable adjust height on the radius of the deposition area. The ring distance from the nozzle and ring diameter was (A) 1 and 2, (B) 2 and 4, and (C) 3 and 6 cm, respectively (Yousefzadeh, 2010) [28]

- The water bath collection device consists of a water bath, where a random mesh of fibers is deposited on the surface and then the fibers are manually directed to the twisting device. This method provides aligned yarns, although the limitations are that the polymer solution must be water-insoluble (some polymers like PCL, poly(vinylidene difluoride) (PVDF), polyvinyl acetate (PVAc), and PAN have shown resistance to dissolve in water), the yield strength of the yarn is low and the size is not uniform. The use of a double bath collection device could enhance the axial alignment

of the yarn. In this method, if auxiliary electrodes are added to the spinneret tip to align the movement of the fibers, it will result in a twisted yarn shape.

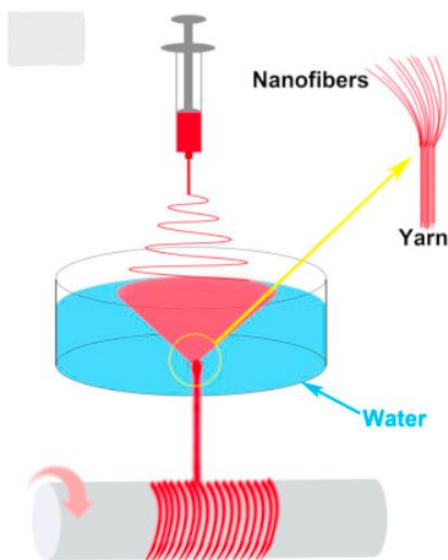


Figure 17: Single water bath collection method, Source: [29]

- The double electrode disc-twisting electrospinning device consists of a uniform electrospinning device with two spinneret heads of opposite charges and a funnel-shaped collector in the middle of them, that creates a hollow cone of fibers at the edge of the funnel. The collector rotates and twists the fibers to form an aligned dry fiber yarn. In case the twisting continues until over-twisting takes place, spiral yarns will be created, which are stronger and highly stretchable.

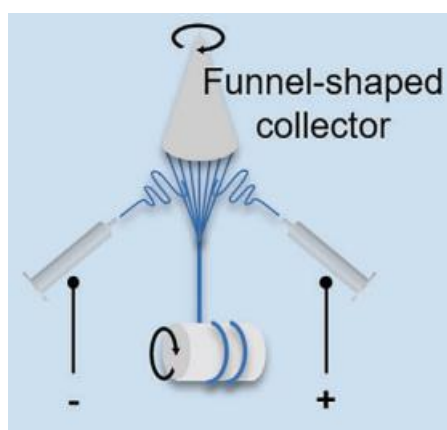


Figure 18: Double electrode disc-twisting electrospinning device, Source: [5]

- Self-collecting spinning technique can produce continuous nanofibers. It consists of a grounded needle tip charged with high voltage and a rotating drum in the base of the needle. The fibers that are ejected from the tip are pulled back and deposited onto the drum collector. This method is simple and has low energy consumption, however, it is challenging to control the self-bundling behavior during the yarn formation, which further leads to low-quality, easily fractured yarns [5].

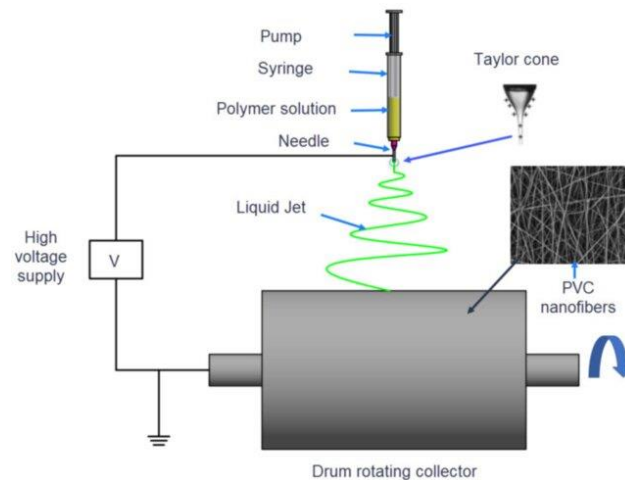


Figure 19: Self-collecting spinning technique, Source: [30]

#### 4.2.2 TWO-DIRECTIONAL

Two-directional are the most used structures due to their large sensing area. They can stand as electronic devices on their own. The mats, depending on their formation process, provide substrates of different orientations and traits, that can be further categorized as in plane or out of plane.

##### i. IN-PLANE STRUCTURES

Concerning the in-plane structures, they can be categorized as random network structures, oriented fiber structures, and patterned structures. In-plane structures may effectively respond to deformation in in-plane directions and displacement in smaller regions while eliminating the possibility of exterior friction fracture.

- The random network structure is shaped with irregular deposition of electrospun fibers onto a mat which creates an entangled porous nanofiber sheet that can be used in flexible/stretchable electronic devices. These devices consist of elastomeric substrates with electrical material depositions. The current polymer

materials used in elastomeric substrates, for instance, polyimide (PI), polydimethylsiloxane (PDMS), rubber, polyethylene terephthalate (PET), latex, or Ecoflex, have inherent mechanical mismatches with most commercially available electrical materials for example metals, or carbon-based materials. Furthermore, they do not allow gas/liquid circulation, which renders them unsuitable for long-term monitoring in on-skin electronics. However, the nanofiber sheets can replace the polymer materials and reduce these effects. They offer great mechanical flexibility and breathability, both important features for wearable skin electronics. Moreover, due to their structure, they hold a high-pore volume and a large surface area, thus they can receive loads of active materials into the substrate. All the above-mentioned characteristics lead to the construction of highly sensitive, flexible, breathable, reshapable, and lightweight devices when utilizing nonconducting electrospun nanofiber sheets as supporting materials [31].

- The oriented fiber mat structure is achieved either by utilizing a roller as a collector or pairs of homogeneously charged electrodes. The first preparation method forms twisted and oriented fibers, similar with those mentioned above, the diameter of which can be controlled by fluctuating the rotational speed of the roller. In the second preparation method, an electrostatically charged oriented flow of the fibers is created between the gaps of the electrode pair (auxiliary electrode pair). The oriented fiber mat exhibits anisotropic tensile behavior, limiting the coupling interference of sensing signals in the other directions, which enhances the sensing performance in the fibers' direction.
- The patterned structure can be attained by methods such as printing of etched material, laser engraving of fiber film, near-field electrospinning, etc. These processes are expensive and not suitable for larger-scale electrospinning.

## ii. OUT-OF-PLANE STRUCTURES

Out-of-plane structures discharge in-plane stresses of the substrate through out-of-plane buckling of nanoscale materials. Stretching of such formations can work in favor of its tensile properties, because of steric buckling. (interaction of ions and molecules in a non-binding way) Their large volume and the out-of-plane buckling structure

make these formations prone to damage by friction. The strain sensors based on these structures usually have a wrinkled, wave-like shape [5].

#### 4.2.3 COMPOSITE STRUCTURES

Composite single fiber structures can be attained by parallel electrospinning, which results in a left-right layered structure with one side co-planar, coaxial or triaxial techniques, using numerous needles, co-electrospinning, using multiple mixed solvent systems or emulsion electrospinning, where various solvents are uniformly dispersed increasing stress transfer and structural integrity. All these methods, clearly separate the substrate from the conductive layer, a fact that might lead to surface detachment issues. To strengthen the adhesion of the substrate to the conductive layer, the substrate can be modified with dopamine (DA) or other accordant compounds. Moreover, composite fibers are obtained when the active agents are dispersed into the liquid polymer solution before the spinning process, and after, a multiphase conductive nanofiber composite is created. These agents limit the plastic deformation in the inverse direction of the fiber orientation- a property that enhances the service life of the sensor. The conductive networks' structural integrity heavily relies on the relative sliding of the active materials. The polymer material acts as a protective and stabilizing layer for the active agents. However, its insulating properties prevent an efficient conductive path from forming between different fibers, and resistance changes are almost exclusively caused by the active material breaking within the same fiber. As a result, the sensor has a poor lower limit of detection and lower sensitivity. The aligned nanofiber layers can be used to create composite materials with exceptional properties. Lee et al, [5] [32] stacked orthogonally (0,90) two aligned carbon nanofiber layers to create a multidirectional strain sensor, achieving a great selectivity of 3.84.

### 4.3 PARAMETERS AFFECTING ELECTROSPINNING

It can be observed, based on the information mentioned above, that the configuration of the devices during the electrospinning process heavily influences the formation of the fibers. These factors are concluded below:

- The number and the set-up of the needles
- The diameter of the needle
- The speed of solution release
- The structure and type of the collector
- The distance of the collector from the spinneret

In addition, the product attained from this process is affected by further factors such as:

- Fluctuations of the electric field
- Environmental factors such as humidity and temperature
- The materials used in the polymer solution- the solvent, the solute, concentrations of each, molecular weights, incorporation of active agents

#### 4.3.1 FLUCTUATIONS OF THE ELECTRIC FIELD

The strength of the electric field is proportional to the voltage applied to it and inversely proportional to the distance from the tip to the collector. A higher strength of the electric field will lead to better-conducting properties of the nanofibers.

#### 4.3.2 ENVIRONMENTAL FACTORS

The humidity and temperature of the environment are important to be controlled, as they affect solvent volatilization and current flow [31].

#### 4.3.3 MATERIAL PROPERTIES

Conductivity, surface tension, viscosity, solvent volatility, molecular weight and molecular structure affect the result of the spinning solution and are distinct characteristics of the materials composing the solution.

A higher conductivity rate implies an increased electrostatic force for the solution when subjected to an electric field, which offers better-stretching qualities and finer fibers. Also, when the solution has a reduced surface tension rate, it benefits the

formation of charged jets and reduces the diameter of the fibers. By choosing a high-conductivity solvent or by adding salt or electrolyte to the solution, both of the above-mentioned qualities can be accomplished.

The viscosity of the solution must also be controlled and it depends on the molecular weight of the polymer and the ratio of the solvent and the polymer. The molecular weight defines the length of the polymeric chain and it needs to be high enough to create fibers. The concentration and electrical conductivity of a polymer solution, in addition to the solvent type and molecular weight of the polymer, are crucial factors that determine its spinnability.

The volatility of a liquid is the indicator of the ease of transforming into a gas. The boiling point of the solvent is interconnected with volatility. The higher the boiling point, the harder it is for the solution to form fibers. The solvent, therefore, should have a low boiling point, in order to be able to evaporate, otherwise, the droplets would not be able to form continuous fibers, but beaded ones [31].

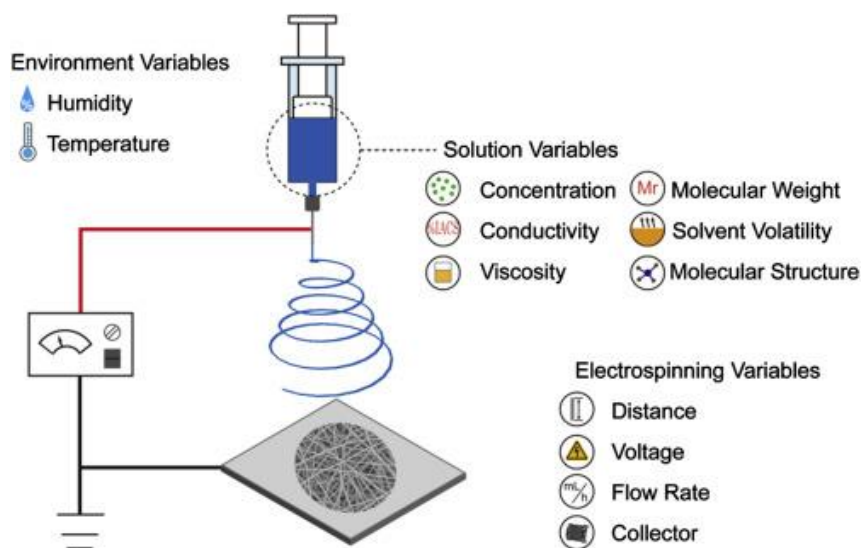


Figure 20: Parameters Affecting the electrospinning process, Source: [33]

#### 4. MATERIALS USED IN ELECTROSPINNING FOR FLEXIBLE STRAIN-SENSORS

The versatility of electrospun fibers allows them to be integrated into strain-sensing structures. Features such as high porosity and high tolerance in stretching of the nanofiber's structure make them great candidates for resistive strain sensors. Their operation mechanism is the production of electrical responses in terms of resistance. This process can provide the best performance of the strain sensor by tuning appropriately the alignment and diameter of the nanofibers. For the accurate measurement of slight deformations on curvilinear or/and dynamic surfaces caused by external factors, the use of durable and highly flexible materials is demanded. As mentioned in Chapter 1, the piezoresistive strain sensors are made of a polymer substrate and a conductive substrate. The polymer substrate consists of insulating elastomeric polymers such as polyacrylonitrile (PAN), polydimethylsiloxane (PDMS), polyurethane (PU), thermoplastic polyurethane (TPU), polyamide (PA), polyvinylidene fluoride (PVDF), polyethylene terephthalate (PET), and polystyrene (PS).

The materials' selection for the polymer solution prior to electrospinning, determines significant characteristics of the fibers, that form the nanofiber mats. Regarding the conductive layer, the polymer solution, that will undergo the electrospinning process, consists of a solvent/or mixture of solvents, a polymer, and sometimes active nanoparticles to provide certain qualities to the nanofibers.

##### 5.1 SOLVENTS

Solvents such as alcohols, chloroform, acetone, dichloromethane, dimethylformamide (DMF), tetrahydrofuran (THF), dimethyl sulfoxide (DMSO), hexafluoroisopropanol (HFIP), and trifluoroethanol are popular choices for electrospinning, however, in some cases it is important to use a mixture of different solvents to achieve the ideal fiber formations. Water has a high dielectric constant, which suppresses the electrostatic repulsion, making it an ineffective choice for this process [24].

## 5.2 POLYMERS

Polymers able to conduct electricity are called conductive. Ordinary polymers, concluding the ones mentioned above, that are produced with the usual methods, typically are insulators. However, there are specific types of conductive polymers depending on the way they attain their conductive properties. Conductive layers of electrospun fibers can be created with four main methods.

- i. By using conductive polymers in fluid form in the solution of the electrospinning process
- ii. By carbonizing polymer electrospun fibers, which are inherently insulating
- iii. By incorporating active nanoparticles into the polymer solution before electrospinning
- iv. By coating the flexible electrospun nanofibers with active nanoparticles.

The first two methods provide fibers with great toughness and the fact that their formation is continuous results in less plastic breakage of the conductive network, yet fewer responses of the sensor in micro strains, and less resistance change. The latter two methods are more complex in their structure; however, they provide highly conductive fibers as a result.

### 5.2.1 CONDUCTIVE POLYMERS

Intrinsically conductive polymers have a structure that, at a molecular level, defines their conductance. They have a rigid backbone consisting of an extensive conjugated system. Further categorization makes up two separate groups, the conductive polymers with conjugated  $\pi$  electrons in the backbone and the doped polymers. In the first group, the conjugated  $\pi$  electrons are responsible for electrical charge. When an electric field is applied conjugated  $\pi$ -electrons can be transported through the solid polymer. Overlapping of orbitals of conjugated  $\pi$  -electrons over the entire backbone leads to the creation of valence bands and conduction bands, which extend over the complete polymer molecule. The presence of conjugated  $\pi$  -electrons in polymers increases its conductivity, e.g., Polypyrrole. In the second group, the conductivity is increased after the polymer is subjected to a charged transfer agent in a gas phase or in solution. Doping can be achieved with two different processes. Either by oxidation, p-Doping, where the polymer is treated with a Lewis acid, or by reduction, n-Doping, treated with a Lewis base [34]. Polymers such as polyaniline (PANI), PA,

polythiophene (PT), polypyrrole (PPy), and its derivatives of poly(3,4-ethylene dioxythiophene) (PEDOT) and poly(3-hexylthiophene) (P3HT), can be used as spinning fluids in the methods of direct electrospinning, co-spinning and electrospun fiber plate synthesis, to create conductive nanofibers. Their final structure is heavily dependent on the method of choice. They can be utilized as functional layers in the strain sensor configuration. Their structural and functioning versatility make them optimal for a wide variety of applications [35] [5] . Their attributes are their abilities to store charges, undergo ion exchanges, be transparent to X-rays, and absorb light in visible frequencies to provide colored products. Nonetheless, their conductivity levels are not as high as those of metals and can be further reduced in storage, they are inflexible and cannot undergo processing, they are unstable at high temperatures, and have low mechanical strength.

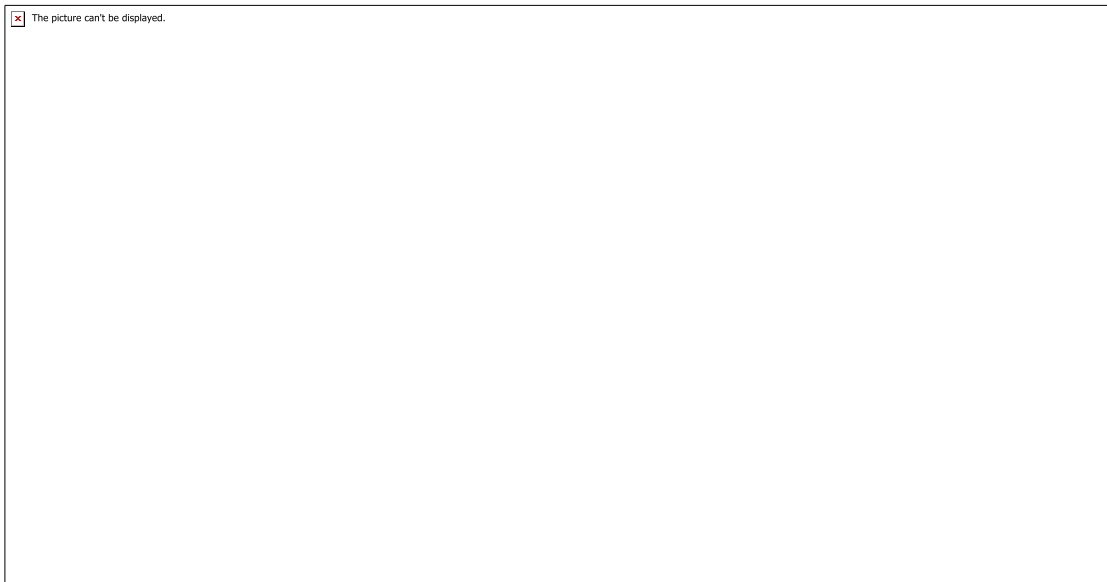


*Figure 21: Conductive polymers in fluid form used in electrospinning for the construction of strain sensors, Source: [35]*

### 5.2.2 CARBONIZATION OF POLYMERS

The process of carbonizing polymer electrospun nanofibers gives them the attribute of conductivity, by creating an interlocking structure of fibers that constitutes the conductive network. Their continuous form offers great stretchability, lower cost, and better control over their structural properties compared to the conductive coating, however, the elastic deformation of the fibers, stabilizes the conductive path and does not allow the detection of micro-strains, which otherwise can be achieved by crack propagation methods of conductive coating with active materials [31]. Katsuya Sode et al, [36] suggested novel electrical conductive carbonized polyimide nanofibers were prepared by a combination of electrospinning and ion-beam irradiation technique. The electrical conductivities of the carbon nanofibers were enhanced with an increase in the ion fluence.

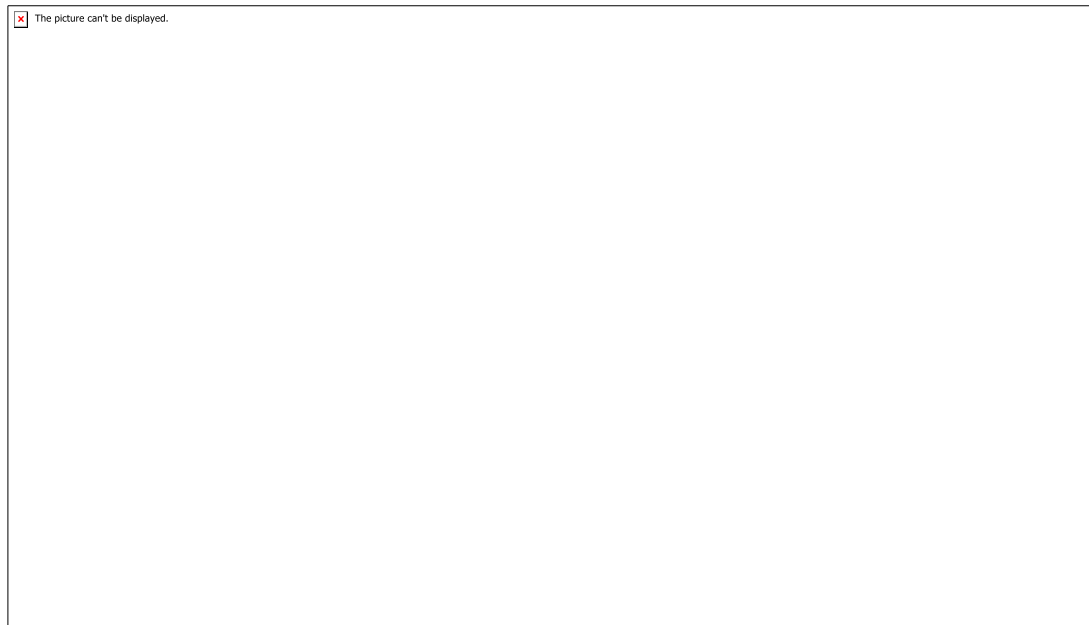


*Figure 22: An example of carbonization of a polymer fiber mat, Source: [36]*

### 5.2.3 BLENDING ACTIVE NANOPARTICLES IN THE ELECTROSPINNING SOLUTION

An appealing material for piezoresistive flexible sensors is a polymer combined with active nanoparticles, used as conductive fillers that have the qualities of flexibility, high conductivity, and mechanical strength. If the filler particles are evenly distributed throughout the matrix, an electron-flowing percolating network will form. The presence of conductive fillers in the flexible layer, allows the conduction path to be connected and disconnected.

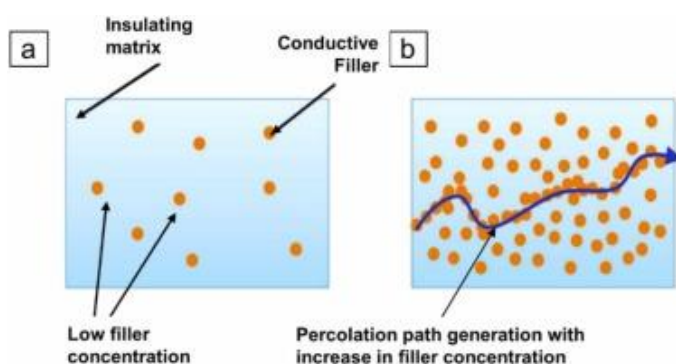


Figure 23: Working Principles of the conductive path that is created due to the conductive fillers in an insulating matrix, Source: [35]

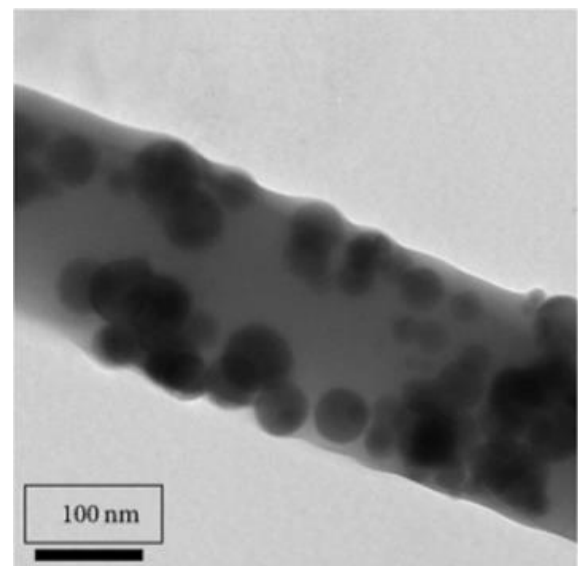


Figure 24: TEM image of CuO nanoparticles in PLGA/CuO electrospun nanofibers, Source: [37]

The conductivity of the polymer nanocomposite above the percolation threshold can be expressed as follows:

$$\sigma = \sigma_0(X - X_c)^B$$

where,  $\sigma$  is the conductivity of the polymer material and the solvent,  $\sigma_0$  is the conductivity of the active nanoparticle added,  $X$  is the volume fraction of the filler,  $X_c$  is the volume fraction of filler at the percolation threshold and  $B$  is the power of conductivity increase after the percolation threshold limit accordingly.

A percolation network is formed at a specific filler concentration, after which conductivity increases exponentially; the filler particles do not need to be in direct

contact, because electrons can tunnel through a small distance, with the tunneling effect [18].

#### 5.2.4 COATING POLYMERS WITH ACTIVE NANOPARTICLES

Extrinsically conducting polymers are conductive because of the presence of externally added active ingredients. Conductive element-filled polymers are one of the subgroups. The conductive elements after being embedded into the polymer solution, by coating methods, remain stable due to the colloidal ability of the polymers. Depending on the element added, e.g. Ag/CNTs/Graphene oxide, the polymer attains analogous qualities. The minimum concentration of the conductive filler that allows the polymer to conduct is called the percolation threshold. The advantages they hold are various. They possess great bulk conductivity and are lightweight, they have significant mechanical strength, are flexible and processable, but also cheaper than intrinsically conductive polymers. All these characteristics make them desirable options as materials for multiple applications such as analytical sensors (for pH, glucose, etc.), microelectronic devices, controlled drug release, biomedical applications, etc [34].

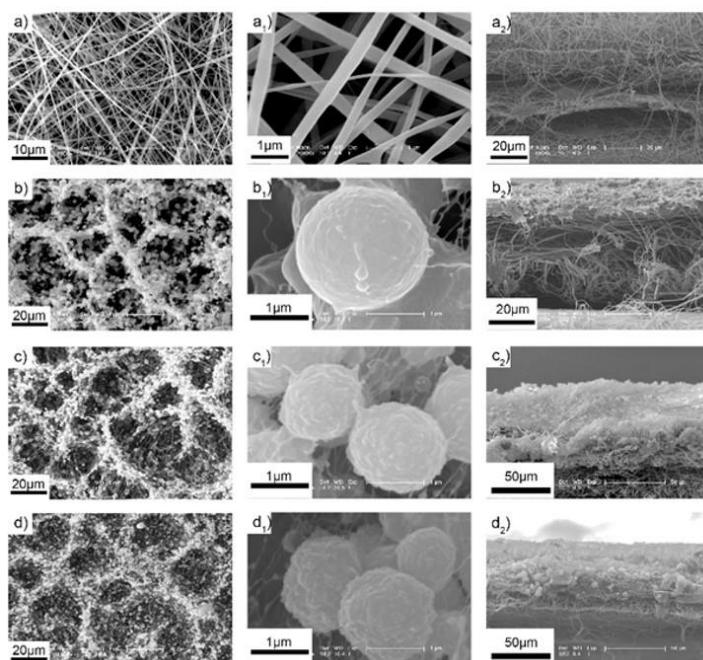


Figure 25 SEM of pure PVDF nanofiber membrane DP8 composite membrane and electrospun DP8-X with different SiO<sub>2</sub> content. (a-a2) PVDF, (b-b2) DP8, (c-c2) DP8-0.5% SiO<sub>2</sub>, (d-d2) DP8-1.0% SiO<sub>2</sub> [Zhang et al 2022]. Source: [37]

## 5. METHODS FOR COATING ELECTROSPUN NANOFIBERS WITH ACTIVE NANOMATERIALS

Active nanomaterials can be introduced in the electrospun fiber substrate with the assistance of specific coating methods, in order to improve the sensitivity of the strain sensor. Scattered active nanomaterials formulate a conductive network, supporting electron transport paths and enhancing conductivity. The choice of material relies on the desired properties and performance of the sensor. Nanoparticles (AuNPs, AgNPs, PtNPs etc.), carbon-based materials (CBs, CTs, GO), nanowires (AgNWs, CuNWs), compound-based materials (ZnO particles, ITO particles,  $\text{MOS}_2$  sheets), liquid metals (LM) or ionic liquids (IL) and composite nanomaterials can all be used to create conductive layers.

Carbon Fibers have considerable mechanical stability and metal nanowires have significant electrical conductivity. Both are most commonly used for flexible strain sensor applications.

There are certain approaches for the preparation of conductive coating films integrated on top of substrates. They are divided into two basic categories, one, in which chemical reactions of some form are included and another one in which only physical interactions take place.

In the first category belong the methods of chemical vapor deposition (CVD), and in situ polymerization.

## 6.1 CHEMICAL VAPOR DEPOSITION

CVD uses reactive substances in gas or vapor form that react directly with the substrate and result in a solid deposit onto it with conductive properties. It is an inexpensive method with a high deposition rate, and great uniformity of the final product layer, though the control of the precise thickness is challenging.

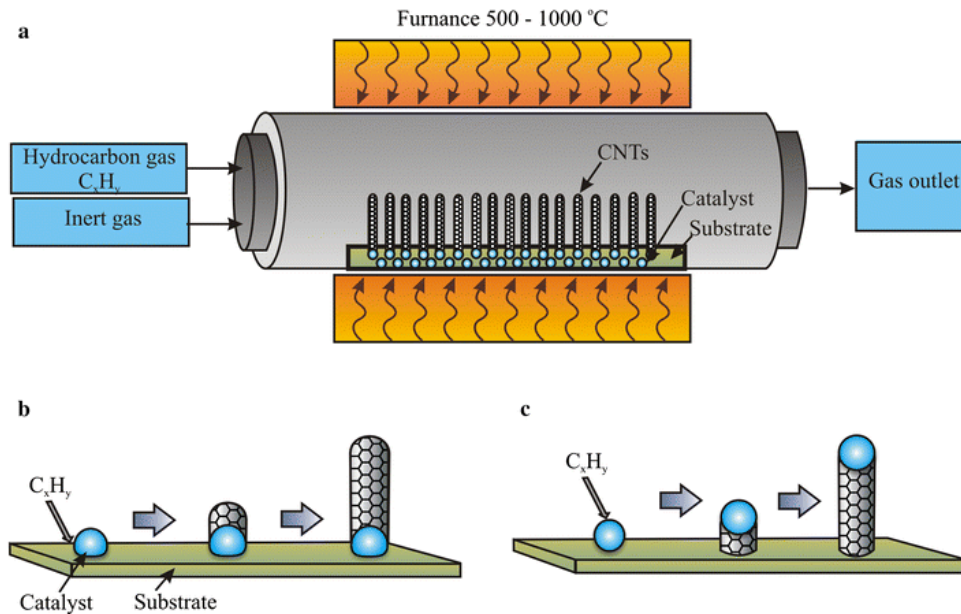


Figure 26: (a) Chemical Vapor Deposition Coating Method, (b) Carbonization, Source: [38]

## 6.2 IN SITU POLYMERIZATION

In situ polymerization involves a solution of reactants in liquid form, where the substrate will be placed, and under specific conditions, chemical reactions are induced. The products of this reaction are deposited straight onto the surface of the substrate. The use of inexpensive ingredients and compatibility with several different heating and curing techniques are a few of the advantages of the in situ polymerization process. However, there are many drawbacks to this preparation technique, such as the scarcity of ingredients that may be used, the short time needed to complete the polymerization process, and the need for costly equipment [39].

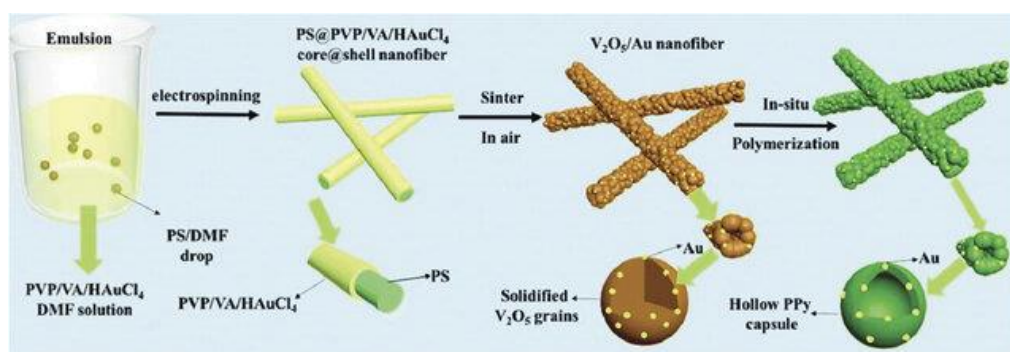


Figure 27: In situ polymerization of hollow Ppy/AuNP fibers, Source: [39]

The second category contains multiple methods with different characteristics for each. Some of the most popular are the Meyer rod, the drop casting, the dip coating and the spraying methods.

### 6.3 MEYER ROD

The Meyer rod is popular in the industry. It is comprised of a stainless-steel rod, wounded tightly with stainless steel wires of various diameters. It controls the coating weight and disposes of excess coating solution. The process is simple and flexible when it comes to active material selection, and it provides good control over the thickness and uniformity of the coating.

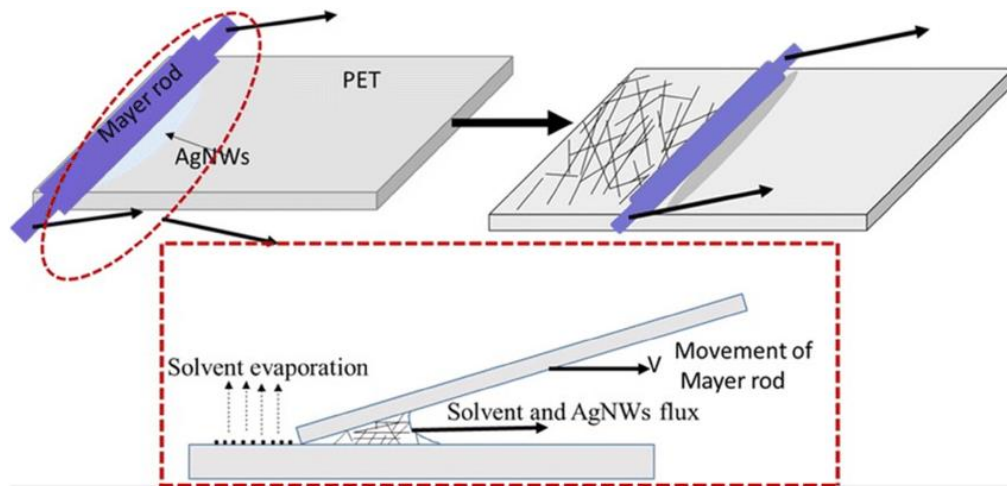


Figure 28: Schematic diagram for fabrication of AgNW-FTCF by Meyer rod [40]

### 6.4 DROP CASTING

Drop casting is a method in which drops concentrating active material are placed onto the substrate. These materials work as electrocatalysts and create a conductive layer. It is a simple, low-cost, and sustainable process, mainly used for the preparation of the conductive layer of strain sensors. However, the uniform thickness of the layer is hard to control, making it not suitable for large areas.

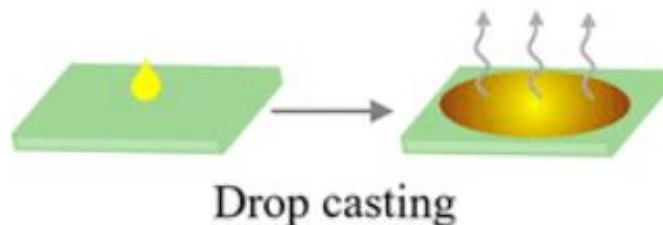


Figure 29: Illustration of Drop-casting coating, Source: [41]

### 6.5 DIP COATING

Dip coating includes sinking the fiber substrate into a dispersed solution of active material. The active material is adhered onto the substrate by ultrasound-assisted treatment which allows deep mixing and reduces interlaminar mismatches, thus producing a tough monolayer structured strain sensor. Although this technique is simple and efficient, it is not appropriate for thin films on intricate surface structures, due to its poor material utilization rate, but it is limited to only producing symmetric coatings.

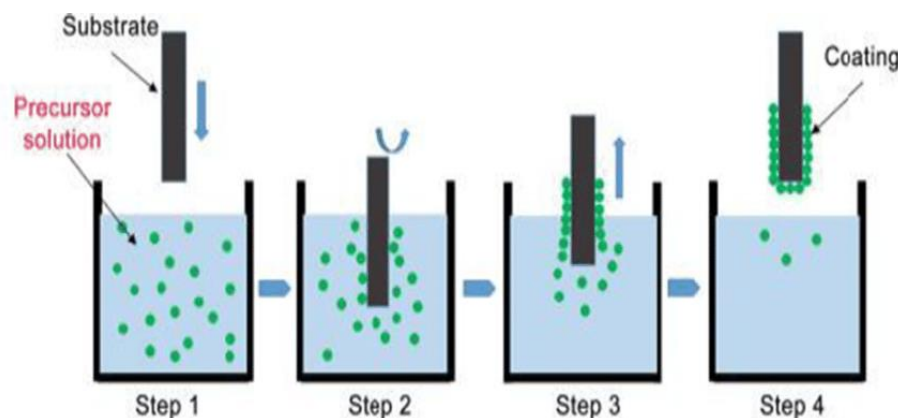


Figure 30: Depiction of the dip coating process, Source: [42]

### 6.6 SPRAY METHOD

The spray method involves spraying an ink made of active materials onto a substrate using a spray gun, to form a conductive coating layer. It holds the benefits of regulated coating thickness, good performance, and easy preparation.

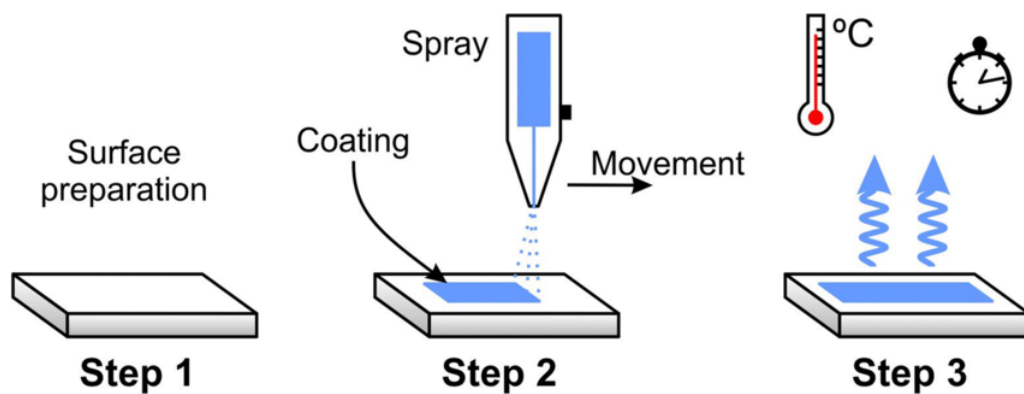


Figure 31: Illustration of the Spray method process, Source: [43]

Other coating methods are:

### 6.7 SPIN COATING METHOD

The spin coating which is a three-step method. It involves dripping, high-speed rotation, and drying curing. It is highly effective and offers great control over the film thickness and uniformity, it is simple and greatly customizable. Nonetheless, it holds issues related to expensive equipment, and inefficient utilization of materials, and faces challenges in producing films on large surface areas.

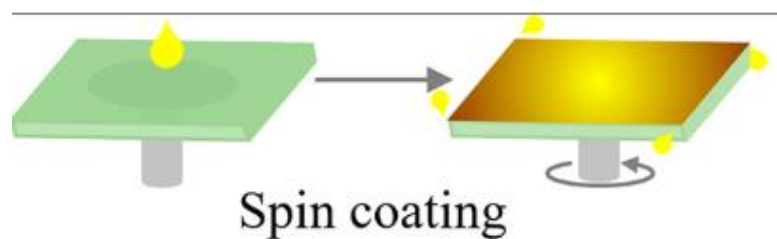


Figure 32: Illustration of the spin coating method, Source: [41]

### 6.8 PRINTING METHOD

The printing technique follows the same principles as the spray method, but the inkjet follows a specific pattern. It is economical and simple, yet it is a slow process with poor pattern resolution and provides non-uniform layers.

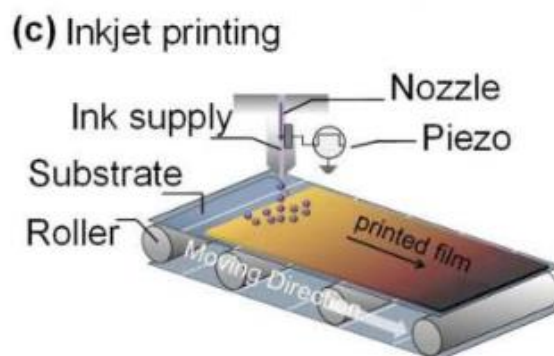


Figure 33: Inkjet printing method, Source: [44]

### 6.9 THERMAL EVAPORATION COATING METHOD

The thermal evaporation coating method is based on heating the active material in the vacuum evaporator and forming a stream that is concentrated onto the substrate surface. Then a curing process follows that results in a solid conductive layer of thin film. This approach provides more uniform films; however, it is not time efficient, has a limited deposition rate, and requires the use of materials with low melting and boiling temperatures.

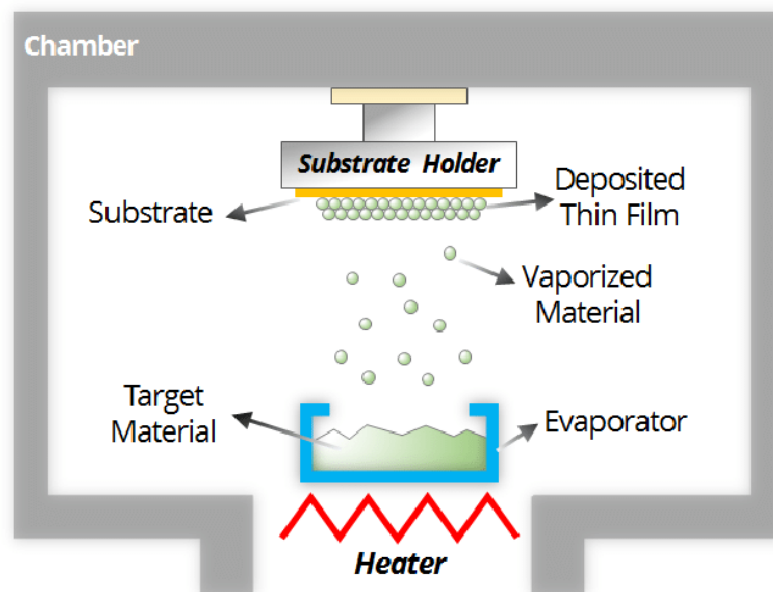


Figure 34: Schematic depiction of the configuration for the thermal evaporation coating method, Source: [45]

## 6.10 SPUTTER COATING METHOD

The sputter coating method's principles are bombarding the target surface with ions and then depositing sputtered active materials on it to produce a conductive layer. The collector's area contains a magnetic field and the process is performed in a vacuum. It promises high purity of the film, yet it is prone to breakage and yield in a low point.

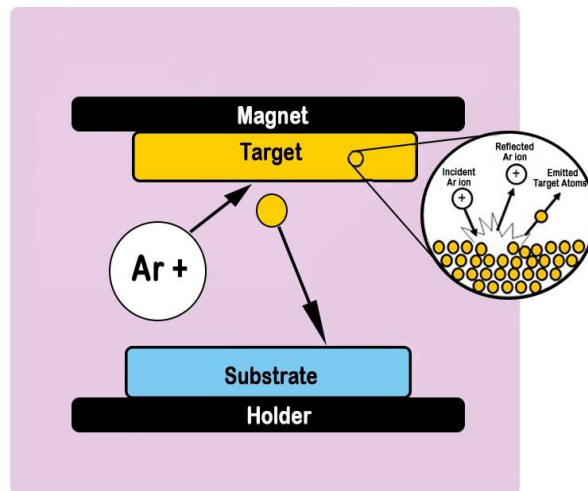


Figure 35: Schematic illustration of the sputter coating method configuration, Source: [46]

### 6.11 VACUUM FILTRATION DEPOSITION METHOD

The vacuum filtration deposition approach achieves the creation of a conductive layer either by transferring the active material suspension straight into the substrate surface while it is under vacuum conditions, or by filtering the desired conductive layer through a microfilter membrane and then laminating it with the substrate with a transfer technique. It requires an initial investment in the equipment and constant energy consumption, and the process must be completed under specific environmental conditions, otherwise, there is a risk of contamination or loss of the final product. In addition, only gas-resistant compounds can be utilized [5].

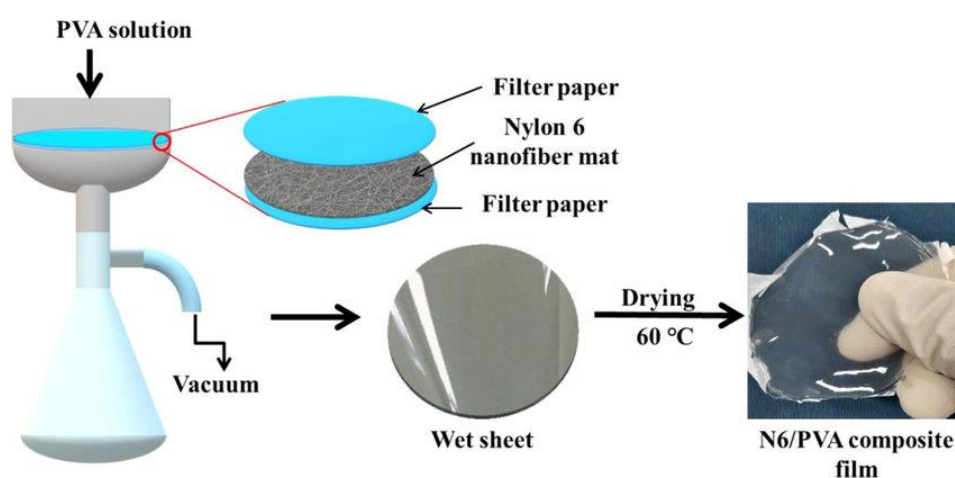


Figure 36: Illustration of a vacuum filtration deposition method with filtration layers, Source: [47]

### 6.12 TRADE OFF

The trade-off method will be utilized to approximately evaluate all the previously mentioned methods. They are scored based on some of their characteristics in the table below. The scoring range is from one (1) to three (3), where one indicates the lowest score for the characteristic, e.g. one in simplicity of manufacturing means that the manufacturing process is very complex, and three showcases the highest score for the characteristic, e.g. three in cost, means that the method is inexpensive.

*Table 2: Trade-off for the active-material coating methods*

<b>Methods</b>	<b>Simplicity</b>	<b>Cost</b>	<b>Time</b>	<b>Thickness control of film</b>	<b>Uniformity of film</b>	<b>Low-waste</b>	<b>Material choice variety</b>	<b>Conductive performance</b>	<b>Total points</b>
Meyer Rod	3	2	2	3	3	1	3	3	20
Drop casting	3	3	2	1	2	3	2	3	19
Dip coating	3	2	3	2	1	1	2	3	17
Spray	3	2	2	3	3	2	2	3	20
Spin coating	3	1	2	3	3	1	3	3	19
Printing	3	3	2	1	1	3	2	2	17
Thermal evaporation coating	2	2	1	2	3	2	1	3	16
Sputter coating	1	1	2	3	3	2	2	3	17
Vacuum filtration deposition	1	3	1	2	2	1	2	3	15
Chemical Vapor Deposition	2	3	2	1	3	2	2	3	18
In situ Polymerization	1	2	3	3	3	2	2	3	19

It can be observed that specific methods collect a noticeably higher score. Meyer Rod method and Spray method have the highest score and Drop casting, Spin coating, and in situ polymerization methods are the ones with the second highest score. In order to decide which one is appropriate for each application, adding a weighting coefficient is important for the characteristics that are of significance in the chosen application.

## CONCLUSION

In summary this literature review has provided a comprehensive exploration on the methods of fabricating flexible strain sensors through the innovative method of electrospinning. The types of flexible strain sensors depending on their transduction mechanism were discussed and accordingly evaluated. The piezoresistive strain sensor was further analyzed and its working principles and performance optimizations were mentioned. Furthermore, the electrospinning method was explained and how its different parameters affect the strain sensor's accuracy. Regarding the trade-off tables, for the evaluations of the types of flexible strain sensors and of the coating methods for active material deposition, the scoring is approximate. In the case that sorting out options is required it is needed to add weighting factors to the most important characteristics on the table depending on the application and the resources. In addition, more characteristics can be introduced. In a possible follow-up research, one can exhibit the structure and material optimizations for the strain sensor, and distinguish which parameters need to be alternated in the electrospinning process in order to obtain the ideal characteristics of the strain sensor depending on the application. The synergy between material science, engineering, and sensor technology showcased fascinating possibilities for the development of highly efficient and adaptable sensing devices.

## REFERENCES

- [1] Jian Tang, Yuting Wu, Shidong Ma, Tao Yan, Zhijuan Pan, Sensing mechanism of a flexible strain sensor developed directly using electrospun composite nanofiber yarn with ternary carbon nanomaterials, *iScience*, Volume 25, Issue 10, 2022
- [2] Zazoum B, Batoor KM, Khan MAA. Recent Advances in Flexible Sensors and Their Applications. *Sensors (Basel)*. 2022 Jun 20;22(12):4653. doi: 10.3390/s22124653. PMID: 35746434; PMCID: PMC9228765
- [3] S. Ma, J. Tang, T. Yan and Z. Pan, "Performance of Flexible Strain Sensors With Different Transition Mechanisms: A Review," in *IEEE Sensors Journal*, vol. 22, no. 8, pp. 7475-7498, 15 April 15, 2022, doi: 10.1109/JSEN.2022.3156286.
- [4] Zhiran Shen, Fanmao Liu, Shuang Huang, Hao Wang, Cheng Yang, Tian Hang, Jun Tao, Wenhao Xia, Xi Xie, Progress of flexible strain sensors for physiological signal monitoring, *Biosensors and Bioelectronics*, 2022, 114298, ISSN 0956-5663, <https://doi.org/10.1016/j.bios.2022.114298>.
- [5] Z. Gao, X. Xiao, A. D. Carlo, J. Yin, Y. Wang, L. Huang, J. Tang, J. Chen, Advances in Wearable Strain Sensors Based on Electrospun Fibers. *Adv. Funct. Mater.* 2023, 33, 2214265. <https://doi.org/10.1002/adfm.202214265> [11]
- [6] Liu, Z., Zhu, T., Wang, J. et al. Functionalized Fiber-Based Strain Sensors: Pathway to Next-Generation Wearable Electronics. *Nano-Micro Lett.* 14, 61 (2022). <https://doi.org/10.1007/s40820-022-00806-8>
- [7] Cai, L., Song, L., Luan, P. et al. Super-stretchable, Transparent Carbon Nanotube-Based Capacitive Strain Sensors for Human Motion Detection. *Sci Rep* 3, 3048 (2013). <https://doi.org/10.1038/srep03048>
- [8] Lee, J., Kwon, H., Seo, J., Shin, S., Koo, J.H., Pang, C., Son, S., Kim, J.H., Jang, Y.H., Kim, D.E. and Lee, T. (2015), Conductive Fiber-Based Ultrasensitive Textile Pressure Sensor for Wearable Electronics. *Adv. Mater.*, 27: 2433-2439. <https://doi.org/10.1002/adma.201500009>
- [9] Lara Natta, Francesco Guido, Luciana Algieri, Vincenzo M. Mastronardi, Francesco Rizzi, Elisa Scarpa, Antonio Quattieri, Maria T. Todaro, Vincenzo Sallustio, and Massimo De Vittorio, Conformable AlN Piezoelectric Sensors as a Non-

invasive Approach for Swallowing Disorder Assessment, ACS Sensors 2021 6 (5), 1761-1769, DOI:10.1021/acssensors.0c02339

[10] Jin, T., Sun, Z., Li, L. et al. Triboelectric nanogenerator sensors for soft robotics aiming at digital twin applications. Nat Commun 11, 5381 (2020). <https://doi.org/10.1038/s41467-020-19059-3>

[11] Dong, K., Peng, X., An, J. et al. Shape adaptable and highly resilient 3D braided triboelectric nanogenerators as e-textiles for power and sensing. Nat Commun 11, 2868 (2020). <https://doi.org/10.1038/s41467-020-16642-6>

[12] Kim, D.W., Lee, J.H., Kim, J.K. et al. Material aspects of triboelectric energy generation and sensors. NPG Asia Mater 12, 6 (2020). <https://doi.org/10.1038/s41427-019-0176-0>

[13] Haotian Chen, Yu Song, Xiaoliang Cheng, Haixia Zhang, Self-powered electronic skin based on the triboelectric generator, Nano Energy, Volume 56, 2019, Pages 252-268, ISSN 2211-2855, <https://doi.org/10.1016/j.nanoen.2018.11.061>.

[14] J.W. Zhong, Q.Z. Zhong, Q.Y. Hu, N. Wu, W.B. Li, B. Wang, B. Hu, J. Zhou, Stretchable Self-Powered Fiber-Based Strain Sensor, Adv. Funct. Mater., 25 (2015), pp. 1798-1803, <https://doi.org/10.1002/adfm.201404087>

[15] Chunjin Wu, Zheng Zhang, Taehoon Kim, Suk Jin Kwon, Kyunbae Lee, Sang-Bok Lee, Moon-Kwang Um, Joon-Hyung Byun, Tsu-Wei Chou, To investigate the effect of bidirectional dimension changes on the sensitivity of magnetic strain sensors, Chemical Engineering Journal, Volume 450, Part 2, 2022, 138088, ISSN 1385-8947, <https://doi.org/10.1016/j.cej.2022.138088>.

[16] Ruixue Sun, Lingxiao Gao, Fenqiang Liu, Hang Su, Lvhua Wu, Zhiyuan Zou, Liangke Wu, Honghui Zhang, Changrong Liao, Magnetically induced robust anisotropic structure of multi-walled carbon nanotubes/Ni for high-performance flexible strain sensor, Carbon, Volume 194, 2022, Pages 185-196, ISSN 0008-6223, <https://doi.org/10.1016/j.carbon.2022.03.032>.

- [17] Sun, H., Fang, X., Fang, Z. *et al.* An ultrasensitive and stretchable strain sensor based on a microcrack structure for motion monitoring. *Microsyst Nanoeng* **8**, 111 (2022). <https://doi.org/10.1038/s41378-022-00419-6>
- [18] Abhinav Sharma, Mohd. Zahid Ansari, Chongdu Cho, Ultrasensitive flexible wearable pressure/strain sensors: Parameters, materials, mechanisms and applications, *Sensors and Actuators A: Physical*, Volume 347, 2022, 113934, ISSN 0924-4247, <https://doi.org/10.1016/j.sna.2022.113934>
- [19] A.I. Oliva-Avilés, F. Avilés, G.D. Seidel, V. Sosa, On the contribution of carbon nanotube deformation to piezoresistivity of carbon nanotube/polymer composites, *Composites Part B: Engineering*, Volume 47, 2013, Pages 200-206, ISSN 1359-8368, <https://doi.org/10.1016/j.compositesb.2012.09.091>.
- [20] Liu, X., Miao, J., Fan, Q. *et al.* Recent Progress on Smart Fiber and Textile Based Wearable Strain Sensors: Materials, Fabrications and Applications. *Adv. Fiber Mater.* **4**, 361–389 (2022). <https://doi.org/10.1007/s42765-021-00126-3>
- [21] Wang, X., Liu, X. & Schubert, D.W. Highly Sensitive Ultrathin Flexible Thermoplastic Polyurethane/Carbon Black Fibrous Film Strain Sensor with Adjustable Scaffold Networks. *Nano-Micro Lett.* **13**, 64 (2021). <https://doi.org/10.1007/s40820-021-00592-9>
- [22] Kartikowati, Christina & Suhendi, Asep & Zulhijah, Rizka & Ogi, Takashi & Iwaki, Toru & Okuyama, Kikuo. (2015). Preparation and evaluation of magnetic nanocomposite fibers containing  $\alpha''$ -Fe<sub>16</sub>N<sub>2</sub> and  $\alpha$ -Fe nanoparticles in polyvinylpyrrolidone via magneto-electrospinning. *Nanotechnology*. **27**. 025601. <https://doi.org/10.1088/0957-4484/27/2/025601>.
- [23] Ambrus, Rita. (2023). Electrospinning of Potential Medical Devices (Wound Dressings, Tissue Engineering Scaffolds, Face Masks) and Their Regulatory Approach. *Pharmaceutics*. **15**. 417. <https://doi.org/10.3390/pharmaceutics15020417>.
- [24] Electrospinning and Electrospun Nanofibers: Methods, Materials, and Applications, Jiajia Xue, Tong Wu, Yunqian Dai, and Younan Xia, *Chemical Reviews* **2019** 119 (8), 5298-5415, DOI: 10.1021/acs.chemrev.8b00593

- [25] Disintegration of water drops in an electric field. *Proceedings of the Royal Society of London Series A Mathematical and Physical Sciences*. 1964;280(1382):383-397. doi:10.1098/rspa.1964.0151
- [26]. Electrically driven jets. *Proceedings of the Royal Society of London A Mathematical and Physical Sciences*. 1969;313(1515):453-475. doi:10.1098/rspa.1969.0205
- [27] Shaohua Wu, Ting Dong, Yiran Li, Mingchao Sun, Ye Qi, Jiao Liu, Mitchell A. Kuss, Shaojuan Chen, Bin Duan, State-of-the-art review of advanced electrospun nanofiber yarn-based textiles for biomedical applications, *Applied Materials Today*, Volume 27, 2022, 101473, ISSN 2352-9407, <https://doi.org/10.1016/j.apmt.2022.101473>.
- [28] M. Yousefzadeh, S. Ramakrishna, Modeling performance of electrospun nanofibers and nanofibrous assemblies, In *Woodhead Publishing Series in Textiles, Electrospun Nanofibers*, Woodhead Publishing, 2017, Pages 303-337, ISBN9780081009079, <https://doi.org/10.1016/B978-0-08-100907-9.00013-1>.
- [29] Jinglei Wu, Yi Hong, Enhancing cell infiltration of electrospun fibrous scaffolds in tissue regeneration, *Bioactive Materials*, Volume 1, Issue 1, 2016, Pages 56-64, ISSN 2452-199X, <https://doi.org/10.1016/j.bioactmat.2016.07.001>.
- [30] Le Quoc, Pham & Uspenskaya, Mayya & Olekhovich, Roman & Olvera Bernal, Rigel. (2021). A Review on Electrospun PVC Nanofibers: Fabrication, Properties, and Application. *Fibers*. 9. 12. <https://doi.org/10.3390/fib9020012>.
- [31] Wang, Y., Yokota, T. & Someya, T. Electrospun nanofiber-based soft electronics. *NPG Asia Mater* 13, 22 (2021). <https://doi.org/10.1038/s41427-020-00267-8>
- [32] J.-H. Lee, J. Kim, D. Liu, F. Guo, X. Shen, Q. B. Zheng, S. Jeon, J.-K. Kim, Highly Aligned, Anisotropic Carbon Nanofiber Films for Multidirectional Strain Sensors with Exceptional Selectivity. *Adv. Funct. Mater.* 2019, 29, 1901623. <https://doi.org/10.1002/adfm.201901623>
- [33] Yun-Ze Long, Xu Yan, Xiao-Xiong Wang, Jun Zhang, Miao Yu, Chapter 2 - Electrospinning: The Setup and Procedure, Editor(s): Bin Ding, Xianfeng Wang,

Jianyong Yu, In Micro and Nano Technologies, Electrospinning: Nanofabrication and Applications, William Andrew Publishing, 2019, Pages 21-52, ISBN 9780323512701, <https://doi.org/10.1016/B978-0-323-51270-1.00002-9>.

[34] Conductive Polymers: Opportunities and Challenges in Biomedical Applications, Toktam Nezakati, Amelia Seifalian, Aaron Tan, and Alexander M. Seifalian, Chemical Reviews 2018 118 (14), 6766-6843

DOI: 10.1021/acs.chemrev.6b00275

[35] Raman, S., Ravi Sankar, A. Intrinsically conducting polymers in flexible and stretchable resistive strain sensors: a review. J Mater Sci 57, 13152–13178 (2022). <https://doi.org/10.1007/s10853-022-07479-z>

[36] Sode, K., Sato, T., Tanaka, M. *et al.* Carbon nanofibers prepared from electrospun polyimide, polysulfone and polyacrylonitrile nanofibers by ion-beam irradiation. *Polym J* **45**, 1210–1215 (2013). <https://doi.org/10.1038/pj.2013.56>

[37] ElectrospinTech, Nanoparticles and nanofiber combination, <http://electrospintech.com/nanoparticlefiber.html>

[38] Zaytseva, Olga & Neumann, Günter. (2016). Carbon nanomaterials: Production, impact on plant development, agricultural and environmental applications. Chemical and Biological Technologies in Agriculture. 3. 10.1186/s40538-016-0070-8.

[39] Xie, Guixu & Cheng, Guoting & Zhu, Dongyang & Yan, Jiashu & Ma, Junqing & Lv, Tianyang & Zhang, Jun & Han, Wenpeng & Long, Yun-Ze. (2021). Progress of Superconducting Nanofibers via Electrospinning. Journal of physics. Condensed matter: an Institute of Physics journal. 34. 10.1088/1361-648X/ac232f.

[40] Wang, Y. & Yang, X. & Du, D. & Zhang, X.. (2019). A comprehensive study of high-performance of flexible transparent conductive silver nanowire films. Journal of Materials Science: Materials in Electronics. 30. 10.1007/s10854-019-01687-1.

[41] Chuantian Zuo, Andrew D. Scully, and Mei Gao, Drop-Casting Method to Screen Ruddlesden–Popper Perovskite Formulations for Use in Solar Cells, ACS Applied Materials & Interfaces 2021 13 (47), 56217, 56225, DOI: 10.1021/acsami.1c17475

- [42] Nwanna, Emeka & Imoisili, Patrick & Jen, Tien-Chien. (2020). Fabrication and synthesis of SnOX thin films: a review. *The International Journal of Advanced Manufacturing Technology*. 111. 1-23. 10.1007/s00170-020-06223-8.
- [43] Frederichi, Diógenes & Scaliante, Mara & Bergamasco, Rosangela. (2021). Structured photocatalytic systems: photocatalytic coatings on low-cost structures for treatment of water contaminated with micropollutants—a short review. *Environmental Science and Pollution Research*. 28. 10.1007/s11356-020-10022-9.
- [44] TechXplore, Printing provskite solar cells by Science China Press, <https://techxplore.com/news/2021-07-perovskite-solar-cells.html>
- [45] Park, Sung-Ik & Quan, Ying-Jun & Kim, Se-Heon & Kim, Hyungsub & Kim, Sooyeun & Chun, Doo-Man & Lee, Caroline & Taya, Minoru & Chu, Won-Shik & Ahn, Sung-Hoon. (2016). A review on fabrication processes for electrochromic devices. *International Journal of Precision Engineering and Manufacturing-Green Technology*. 3. 397-421. 10.1007/s40684-016-0049-8.
- [46] LinkedIn, Sputtering Process| Sputtering Deposition Method, Vac Coat, <https://www.linkedin.com/pulse/sputtering-process-deposition-method-vac-coat/>
- [47] Gavande, Vishal & Im, Donghyeok & Jin, Youngup & Lee, Won-Ki. (2021). Fabrication of toughest and transparent electrospun nylon 6 nanofiber-reinforced PVA composites. *Molecular Crystals and Liquid Crystals*. 729. 1-7. 10.1080/15421406.2021.1946985.
- [48] Ghosh, S. K., Adhikary, P., Jana, S., Biswas, A., Sencadas, V., Gupta, S. D., ... & Mandal, D. (2017). Electrospun gelatin nanofiber based self-powered bio-e-skin for health care monitoring. *Nano Energy*, 36, 166-175.

## APPENDIX

### Conductivity

The ability of the material to conduct electric current. It is inversely proportional to resistivity. The SI unit is Siemens/m. It is symbolized with  $\sigma=1/\rho$  where  $\rho$ =resistivity.

### Surface tension

Surface tension is the tendency of liquid surfaces at rest to shrink into the minimum surface area possible. Surface tension, represented by the symbol  $\gamma$  (alternatively  $\sigma$  or  $T$ ), is measured in force per unit length. Its SI unit is newton per meter.  $\gamma = F/(2*L)$

### Viscosity

Usually referred to as the dynamic viscosity. It is the measure of resistance to deformation of a fluid at a given rate. It is the material property that relates the viscous stresses (stresses caused by deformation rate over time) to the strain rate.

Dynamic viscosity is often symbolized with  $\mu$  or  $\eta$  and it has units in SI  $[\mu]= \text{kg}/(\text{m}^*\text{s}) = \text{N}^*\text{s}/\text{m}^2 = \text{Pa}^*\text{s}$  and it is a measure of pressure multiplied by time. Kinematic viscosity is symbolized with  $\nu$  and is a measure of specific energy multiplied by time and it's analogous to dynamic viscosity, governed by the relation:  $\nu=\mu/\rho$ . Its SI units are  $[\nu]= \text{m}^2/\text{s} = \text{N}^*\text{m}^*\text{s}/\text{kg} = \text{J}^*\text{s}/\text{kg}$